Reduced growth with increased quotas of particulate organic and inorganic carbon in the coccolithophore *Emiliania huxleyi* under future ocean climate change conditions

Yong Zhang,[1,4] Sinéad Collins,[2] Kunshan Gao[1,3,*]

[1]State Key Laboratory of Marine Environmental Science and College of Ocean and Earth Sciences, Xiamen University, Xiamen, China

[2]Institute of Evolutionary Biology, School of Biological Sciences, University of Edinburgh, Edinburgh EH9 3FL, United Kingdom

[3]Co-Innovation Center of Jiangsu Marine Bio-industry Technology, Jiangsu Ocean University, Lianyungang, China

[4]College of Environmental Science and Engineering, and Fujian Key Laboratory of Pollution Control and Resource Recycling, Fujian Normal University, Fuzhou, China

Running head: Response of *E. huxleyi* to multiple drivers

[*]Correspondence: Kunshan Gao (ksgao@xmu.edu.cn)

Keywords: CO_2; coccolithophore; functional trait plasticity; light; multiple drivers; nutrients; ocean acidification; warming.

Abstract

Effects of ocean acidification and warming on marine primary producers can be modulated by other environmental factors, such as levels of nutrients and light. Here, we investigated the interactive effects of five oceanic environmental drivers (CO_2, temperature, light, dissolved inorganic nitrogen and phosphate) on growth rate, particulate organic (POC) and inorganic (PIC) carbon quotas of the cosmopolitan coccolithophore *Emiliania huxleyi*. Population growth rate increased with increasing temperature (16 to 20 °C) and light intensities (60 to 240 µmol photons m^{-2} s^{-1}), but decreased with elevated pCO_2 concentrations (370 to 960 µatm) and reduced availability of nitrate (24.3 to 7.8 µmol L^{-1}) and phosphate (1.5 to 0.5 µmol L^{-1}). POC quotas were predominantly enhanced by combined effects of increased pCO_2 and decreased availability of phosphate. PIC quotas increased with decreased availability of nitrate and phosphate. Our results show that concurrent changes in nutrient concentrations and pCO_2 levels predominantly affected growth, photosynthetic carbon fixation and calcification of *E. huxleyi*, and imply that plastic responses to progressive ocean acidification, warming and decreasing availability of nitrate and phosphate reduce population growth rate while increasing cellular quotas of particulate organic and inorganic carbon of *E. huxleyi*, ultimately affecting coccolithophore-related ecological and biogeochemical processes.

1 Introduction

Ocean acidification (OA), due to continuous oceanic absorption of anthropogenic CO_2, is occurring alongside ocean warming. This in turn, leads to shoaling in the upper mixed layer (UML) and a consequent reduction in the upward transport of nutrients into the UML. These ocean changes expose phytoplankton cells within the UML to multiple simultaneous stressors or drivers, and organismal responses to these drivers can affect both trophic and biogeochemical roles of phytoplankton (see reviews by Boyd et al., 2015; Gao et al., 2019 and literatures therein). While most studies on the effects of ocean global climate changes on marine primary producers have focused on organismal responses to one, two or three environmental drivers, there is an increasing awareness of the need to measure the combined effects of multiple drivers (see reviews by Riebesell and Gattuso, 2015; Boyd et al., 2018; Gao et al., 2019; Kwiatkowski et al., 2019). For this purpose, several manipulative experimental approaches have been recommended (Boyd et al., 2018). One approach using many unique combinations of different numbers of drivers showed that both short and long-term growth responses were, on average, explained by the dominant single driver in a multi-driver environment, but this result relies on having many (>5) drivers with known or measured large-effect single drivers (Brennan and Collins, 2015; Brennan et al., 2017). For experiments with multiple drivers where interactions are likely to preclude making predictions from single drivers, where average responses are not the most informative ones, or where logistics preclude using a very large number of multi-driver environments, Boyd et al. (2010) suggested an 'environmental cluster' method where key drivers (such as temperature, light intensity, nutrient concentration, CO_2 and Fe) are covaried within experiments, allowing the investigation of physiological responses of phytoplankton to concurrent changes of the clustered

76 drivers. This approach examines responses to projected overall environmental shifts
77 rather than pulling apart the biological or statistical interactions between responses to
78 individual drivers. To our knowledge, studies to date have employed such a driver
79 clustering approach to investigate responses of diatoms *Fragilariopsis cylindrus*,
80 *Thalassiosira pseudonana*, *Skeletonema costatum*, and the prymnesiophyte
81 *Phaeocystis antarctica* to combinations of drivers projected for 2100 (Xu et al., 2014a;
82 Xu et al., 2014b; Boyd et al., 2016).

83 An environmental cluster approach is especially useful when drivers are known to
84 interact in terms of the organismal responses they elicit, as is the case for OA, light
85 levels, and key nutrients acting on population growth rate and carbon fixation (Boyd
86 et al., 2016). For example, in the cosmopolitan coccolithophore *Emiliania huxleyi*,
87 interactive effects of OA and light showed that OA increased population growth rate
88 and photosynthetic carbon fixation under low light, whereas it slightly lowered
89 population growth rate and photosynthetic carbon fixation under high light
90 (Zondervan et al., 2002; Kottmeier et al., 2016). In addition, photosynthetic carbon
91 fixation was further enhanced by longer light exposure at high pCO_2 levels
92 (Zondervan et al., 2002). On the other hand, OA can exacerbate the negative impact
93 of solar UV radiation on photosynthetic carbon fixation and calcification in *E. huxleyi*
94 under nutrient-replete conditions (Gao et al., 2009), but can increase calcification
95 (coccolith volume) and particulate organic carbon (POC) quota under phosphate-
96 limited conditions (Leonardos and Geider, 2005; Müller et al., 2017), demonstrating
97 that the effects of OA on calcification is likely nutrient-dependent. On the other hand,
98 ocean warming, which occurs alongside OA, is known to increase coccolith length,
99 POC, particulate organic nitrogen (PON) and inorganic carbon (PIC) production rates
100 of several *E. huxleyi* strains (Rosas-Navarro et al., 2016; Feng et al., 2017). Warming

101 has also been shown to increase the optimal pCO_2 levels for growth, POC and PIC
102 production rates (Sett et al., 2014). In one case warming was found to compensate for
103 the negative impact of OA on growth rate under low light intensity (Feng et al., 2008).
104 Nevertheless, decreased photosynthetic carbon fixation and calcification at reduced
105 carbonate saturation state (lowered Ca^{2+} concentrations) were exacerbated by
106 warming treatment (Xu et al., 2011). Overall, there is strong evidence that
107 understanding the plastic responses of this key calcifier to ocean changes requires
108 investigating responses to the overall expected shift in the environment, in addition to
109 the detailed studies to date on individual drivers, due to the sheer number of
110 interactions between individual drivers on traits that affect the trophic and
111 biogeochemical roles of *E. huxleyi.*

112 Despite known interactions among two- and three-way combinations of OA,
113 temperature, light, phosphate levels and nitrogen levels, there have been few
114 empirical studies investigating effects of the larger cluster projected for future surface
115 ocean changes. The data to date show that interactions among drivers can affect both
116 the direction and magnitude of trait changes in biogeochemically important taxa. In
117 addition, based on single or two-driver studies, changes in temperature, pCO_2, light,
118 dissolved inorganic nitrogen (DIN) and phosphate (DIP) in combination are predicted
119 to affect primary productions (Barton et al., 2016; Monteiro et al., 2016; Boyd et al.,
120 2018; Gao et al., 2019; Kwiatkowski et al., 2019). Understanding the trait-based
121 responses of cocolithophores to future ocean changes is important for projections of
122 changes in the biogeochemical roles of phytoplankton, such as biological carbon
123 pump efficiency (Rost and Riebesell, 2004).

124 In order to understand the combined effects of pCO_2, temperature, light, dissolved
125 inorganic nitrogen (DIN) and phosphate (DIP) on functional traits, we incubated

126 *Emiliania huxleyi* (Lohmann) under different combinations of environmental
127 conditions that represented subsets of, and eventually the complete set of
128 environments for, this environmental driver cluster. We recently examined the
129 interactive effects of light intensity and CO_2 level on growth rate, POC and PIC
130 quotas of *E. huxleyi* under nutrients replete, low DIN, or low DIP concentrations
131 (Zhang et al., 2019). Light, CO_2, DIN and DIP levels usually change simultaneously
132 with temperature, and temperature modulated responses of *E. huxleyi* to other
133 environmental drivers (Gafar and Schulz, 2018; Tong et al., 2019). In addition,
134 warming or cooling can direcly influence the activity of enzymes, thus directly
135 modulating metabolic rates (Sett et al., 2014). Because of the overwhelming evidence
136 that temperature can act as a general modulator of organismal responses, we use the
137 present study to examine how the addition of temperature as a key driver in the
138 environmental change cluster can modulate the combined effects of CO_2, light and
139 nutrients. We found that future ocean scenario treatments with OA, warming,
140 increased light and reduced availability of nutrients led to lower growth rate and
141 larger POC and PIC quotas of *E. huxleyi*.
142

143 **2 Materials and Methods**

144 **2.1 Experimental setup**

145 *Emiliania huxleyi* strain PML B92/11 was originally isolated from coastal waters off
146 Bergen, Norway, and obtained from the Plymouth algal culture collection, UK. The
147 average levels of pCO_2, temperature, light, dissolved inorganic nitrate (DIN) and
148 phosphate (DIP) were set up according to recorded data in Norwegian coastal waters
149 during 2000 to 2007 and projected for 2100 in high-latitudes (Larsen et al., 2004;
150 Locarnini et al., 2006; Omar et al., 2010; Boyd et al., 2015) (Table S1). *E. huxleyi* was

151 cultured with a 12 h/12 h light/dark cycle in thermo-controlled incubators in Aquil
152 medium, which was prepared according to Sunda et al. (2005) with the addition of
153 2200 μmol L^{-1} bicarbonate to achieve the total alkalinity (TA) of 2200 μmol L^{-1}.
154 Initial DIN and DIP concentrations were 24 μmol L^{-1} and 1.5 μmol L^{-1}, respectively,
155 and initial light intensity was 60 μmol photons m^{-2} s^{-1}. The experiment was conducted
156 in five steps (Fig. 1). Considering ocean acidification and warming as the key drivers
157 for ocean climate changes, we first established 4 "baseline" treatments where the
158 pCO_2 and temperature drivers were combined in a fully factorial way: low pCO_2 +
159 low temperature (LCLT), high pCO_2 + low temperature (HCLT), low pCO_2 + high
160 temperature (LCHT), and high pCO_2 + high temperature (HCHT). Since reduced
161 availability of nutrients and increased light exposures are triggered by warming-
162 enhanced stratification, we then added additional single or pairs of drivers to each of
163 these "baseline" treatments (Fig. S1). In step 1, low light (LL, 60 μmol photons m^{-2} s^{-}
164 ^{1}) was supplied; in step 2, high light (HL, 240 μmol photons m^{-2} s^{-1}) was exposed. HL
165 was then maintained for the rest of the experiment. In step 3, low nitrogen was
166 supplied and high phosphate levels were maintained (LNHP). In step 4, low
167 phosphate was used and high nitrogen levels were restored (HNLP). In step 5, both
168 nitrogen and phosphate were low (LNLP), respectively (Figs. 1 and S1). In all cases,
169 the cells were acclimated to each unique stressor cluster for at least 14–16 generations
170 before physiological and biochemical parameters were measured. Although this
171 stepwise design introduces a historical effect, physiological traits are generally
172 reported after 10 to 20 generations acclimation to OA treatment (Perrin et al., 2016;
173 Tong et al., 2016; Li et al., 2017), so the historical effects here are similar to those that
174 would be introduced with standard methods in other physiology studies (Tong et al.,
175 2016; Zhang et al., 2019). Since individually reduced availability of nitrate or

176 phosphate decreased growth, did not change POC quota, and enhanced PIC quota
177 under optimal light intensity (HL in this study) in the same *E. huxleyi* strain (Zhang et
178 al., 2019), we hypothesized that combination of DIN and DIP limitation would result
179 in similar trend under the pCO_2 and/or temperature combined treatments. Therefore,
180 we added stepwise nitrate and/or phosphate drivers (Fig. 1). Such stepwise reduction
181 of nutrients levels would be useful for us to analyze effects of nitrate and phosphate
182 separately, and be expected to have implications for the cells episodically exposed to
183 different levels of nutrients in the sea.

184 For step 1, NO_3^- and PO_4^{3-} were modified to 24 μmol L^{-1} and 1.5 μmol L^{-1},
185 respectively, which is the HNHP treatment in the synthetic seawater (Sunda et al.,
186 2005) (Fig. S1). The seawater was dispensed into 4 glass bottles, and 2 bottles of
187 seawater were placed at 16 °C (LT) in an incubator (HP400G-XZ, Ruihua, Wuhan),
188 and aerated for 24 h with filtered (PVDF 0.22 μm pore size, Haining) air containing
189 400 μatm (LC) or 1000 μatm pCO_2 (HC). Another 2 bottles of seawater were
190 maintained at 20 °C (HT) in the other chamber and also aerated with LC or HC air as
191 described above. The dry air/CO_2 mixture was humidified with deionized water prior
192 to the aeration to minimize evaporation. The LCLT, HCLT, LCHT and HCHT
193 seawaters (Figs. 1a and S1) were then filtered (0.22 μm pore size, Polycap 75 AS,
194 Whatman) and carefully pumped into autoclaved 250 mL polycarbonate bottles
195 (Nalgene, 4 replicate flasks for each of LCLT, HCLT, LCHT and HCHT, a total of 16
196 flasks at the beginning of the experiment) with no headspace to minimize gas
197 exchange. The flasks were inoculated at a cell density of about 150 cells mL^{-1}. The
198 volume of the inoculum was calculated (see below) and the same volume of seawater
199 was taken out from the bottles before inoculation. The samples were initially cultured
200 at 60 μmol photons m^{-2} s^{-1} (LL) of photosynthetically active radiation (PAR)

201 (measured using a PAR Detector, PMA 2132 from Solar Light Company) under
202 LCLT, HCLT, LCHT and HCHT conditions for 8 generations (6 days) (d), and then
203 the samples were diluted to their initial concentrations and grown for another 8
204 generations (6 d) (Fig. 1a). Samples in culture bottles were mixed twice a day at 9:00
205 a.m. and 5:00 p.m. At the end of the incubation, sub-samples were taken for
206 measurements of cell concentration, POC and TPC quotas, TA, pH and nutrient
207 concentrations.

208 In step 2, samples grown under the previous conditions were transferred at the end
209 of the cultures from 60 (LL) to 240 μmol photons m^{-2} s^{-1} (HL) of PAR with initial cell
210 concentrations of 150 cells mL^{-1}, and acclimated to the HL for 8 generations (5 d in
211 16 °C environment, 4 d in 20 °C environment) (Fig. 1b). The cultures were then
212 diluted to achieve initial cell concentration and incubated at the HL for another 8
213 generations (the fifth day in 16 °C environment and the fourth day in 20 °C
214 environment) before sub-samples were taken for measurements.

215 In step 3, step 4 and step 5, NO_3^- and PO_4^{3-} concentrations were set to be 8 μmol L^{-}
216 ^{1} and 1.5 μmol L^{-1} for the LNHP treatment, and 24 μmol L^{-1} and 0.5 μmol L^{-1} for the
217 HNLP treatment, and 8 μmol L^{-1} and 0.5 μmol L^{-1} for the LNLP treatment,
218 respectively (Fig. 1c,d,e). The LCLT, HCLT, LCHT and HCHT were step 1
219 conditions, now we are into step 3, 4 and 5. Under 240 μmol photons m^{-2} s^{-1} (HL) of
220 PAR, cell samples with an initial concentration of 150 cells mL^{-1} were transferred
221 from HNHP condition (step 2) to LNHP conditions (step 3) and acclimated to LNHP
222 conditions for 8 generations (5 d in 16 °C environment, 4 d in 20 °C environment)
223 (Fig. 1c). The cultures were then diluted back to initial cell concentrations and
224 incubated in the LNHP conditions (step 3) for a further 8 generations. On the last day

225 of the incubation (the fifth day in 16 ºC environment and the fourth day in 20 ºC
226 environment), sub-samples were taken for measurements of the parameters.

227 After that, cell samples were transferred stepwise from HNHP conditions (step 2,
228 Fig. 1b) to HNLP conditions (step 4, Fig. 1d), then from HNLP conditions to LNLP
229 conditions (step 5, Fig. 1e). Cell samples were acclimated for 8 generations at HNLP
230 and LNLP conditions, respectively, and followed by another 8 generation incubations
231 for 4 d at HT and 5 d at LT. On the fourth day (for populations in high temperature
232 environments) or the fifth day (for populations in low temperature environments),
233 sub-samples were taken for measurements (Fig. 1d,e). At low nutrient concentrations,
234 maximal cell concentrations were limited by nutrients (Rouco et al., 2013; Rokitta et
235 al., 2016). To check whether cells sampled were in exponential growth at each
236 nutrient level, we examined cell concentrations every day at LCHT, or LCLT and
237 high light conditions (Fig. S2). We found that cell concentrations were in the
238 exponential growth phase during the 1st and 5th days at HT, and during the 1st and 7th
239 days at LT. In this study, we took samples in the 4th day at HT and in the 5th day at LT,
240 and thus cells sampled were in the exponential growth phase of *E. huxleyi*.

241 In the previous work (Zhang et al., 2019), we transferred *E. huxleyi* cells stepwise
242 from 80 μmol photons m^{-2} s^{-1} to 120 μmol photons m^{-2} s^{-1}, then to 200 μmol photons
243 m^{-2} s^{-1}, to 320 μmol photons m^{-2} s^{-1} and to 480 μmol photons m^{-2} s^{-1} at both LC and
244 HC levels under HNHP, LNHP or HNLP conditions, respectively. In this study, we
245 transferred the same strain from LL to HL under HNHP condition, and then from
246 HNHP to LNHP or HNLP, and from HNLP to LNLP under HL conditions under 4
247 "baseline" CO_2 and temperature treatments, in an effort to elucidate interactive and
248 combined effects of temperature, CO_2, DIN and DIP (Table S2), in contrast the
249 previous work carried out under constant temperature (Zhang et al., 2019).

250

251 **2.2 Nutrient concentrations and carbonate chemistry measurements**

252 In the first and last days of the incubations, 20 mL samples for determination of
253 inorganic nitrogen and phosphate concentrations were taken at the same time using a
254 filtered syringe (0.22 μm pore size, Haining) and measured by using a scanning
255 spectrophotometer (Du 800, Beckman Coulter) according to Hansen and Koroleff
256 (1999). The nitrate was reduced to nitrite by zinc cadmium reduction and then total
257 nitrite concentration was measured. In parallel, 25 mL samples were taken for
258 determination of total alkalinity (TA) after being filtered (0.22 μm pore size, Syringe
259 Filter) under moderate pressure using a pump (GM-0.5A, JINTENG) and stored in the
260 dark at 4 ^{o}C for less than 7 d. TA was measured at 20 ^{o}C by potentiometric titration
261 (AS-ALK1+, Apollo SciTech) according to Dickson et al. (2003). Samples for pH_T
262 (total scale) determinations were syringe-filtered (0.22 μm pore size), and the bottles
263 were filled from bottom to top with overflow and closed immediately without
264 headspace. The pH_T was immediately measured at 20 ^{o}C by using a pH meter
265 (Benchtop pH, Orion 8102BN) which was calibrated with buffers (Tris•HCl, Hanna)
266 at pH 4.01, 7.00 and 10.00. Carbonate chemistry parameters were calculated from TA,
267 pH_T, phosphate (at 1.5 μmol L^{-1} or 0.5 μmol L^{-1}), temperature (at 16 ^{o}C or 20 ^{o}C), and
268 salinity using the CO_2 system calculation in MS Excel software (Pierrot et al., 2006).
269 K_1 and K_2, the first and second carbonic acid constants, were taken from Roy et al.
270 (1993).

271

272 **2.3 Cell concentration measurements**

273 In the last day of the incubation, ~25 mL samples (8 samples) were taken at the same
274 time (about 1:00 p.m.). Cell concentration and cell diameter (D) were measured using

275 a Z2 Coulter Particle Count and Size Analyzer (Beckman Coulter). The diameter of
276 detected particles was set to be 3 to 7 μm in the instrument, which excludes detached
277 coccoliths (Müller et al., 2012). Cell concentration was also measured by microscopy
278 (ZEISS), and variation in measured cell concentration between two methods was ±
279 7.9% (Zhang et al., 2019). Average growth rate (μ) was calculated for each replicate
280 according to the equation: $\mu = (\ln N_1 - \ln N_0) / d$, where N_0 was 150 cells mL^{-1} and N_1
281 was the cell concentration in the last day of the incubation, d was the growth period in
282 days. *E. huxleyi* cells were spherical and its cell volume with coccoliths was
283 calculated according to the equation: $V = 3.14 \times (4/3) \times (D/2)^3$.
284

285 **2.4 Total particulate (TPC) and particulate organic (POC) carbon measurements**

286 100 mL samples for determination of TPC and POC quotas were filtered onto GF/F
287 filters (pre-combusted at 450 °C for 6 h) at the same time in each treatment. TPC and
288 POC samples were stored in the dark at –20 °C. For POC measurements, samples
289 were fumed with HCl for 12 h to remove inorganic carbon, and samples for TPC
290 measurements were not treated with HCl. All samples were dried at 60 °C for 12 h,
291 and analyzed using a Thermo Scientific FLASH 2000 CHNS/O elemental analyzer
292 (Thermo Fisher, Waltham, MA). Particulate inorganic carbon (PIC) quota was
293 calculated as the difference between TPC quota and POC quota. POC and PIC
294 production rates were calculated by multiplying cellular contents with μ (d^{-1}),
295 respectively. Variations in measured carbon content between the four replicates were
296 calculated to be 1–24% in this study.
297

298 **2.5 Data analysis**

299 Firstly, we examined the interactions of temperature, pCO_2 and light under nutrient-
300 replete (HNHP) conditions. Here, the effects of temperature, pCO_2, light intensity and
301 their interaction on growth rate, POC and PIC quotas were tested using a three-way
302 analysis of variance (ANOVA). Secondly, we examined the effects of nutrient
303 limitation in the different pCO_2 and temperature environments under the high light
304 intensity (HL). Here, the effects of temperature, pCO_2, dissolved inorganic nitrogen
305 (DIN), dissolved inorganic phosphate (DIP) and their interaction on growth rate, POC
306 and PIC quotas were tested using a four-way ANOVA. Finally, a one-way ANOVA
307 was used to test the differences in growth rate, POC and PIC quotas between present
308 (defined as low levels of pCO_2, temperature and light along with high levels of DIN
309 and DIP (LC LT LL HN HP)) and future ocean (defined as higher levels of pCO_2,
310 temperature, and light along with low levels of DIN and DIP (HC HT HL LN LP))
311 scenarios. A Tukey post hoc test was performed to identify the differences between
312 two temperatures, two pCO_2 levels, two DIN or two DIP treatments. Normality of
313 residuals was conducted with a Shapiro-Wilk's test, and a Levene test was conducted
314 graphically to test for homogeneity of variances. A generalized least squares (GLS)
315 model was used to stabilize heterogeneity if variances were non-homogeneous. All
316 statistical calculations were performed using *R* (R version 3.5.0).

317 In order to quantify the individual effect of nitrate concentration or phosphate
318 concentration on the physiological and biochemical parameters, we calculated the
319 change ratio (R) of physiological rates according to the equation: $R = |M_{\text{LNHP or HNLP}}$
320 $- M_{\text{HNHP}}| / M_{\text{HNHP}}$, where $M_{\text{LNHP or HNLP or HNHP}}$ respresents measured trait values in
321 LNHP or HNLP or HNHP conditions, and the '|' denotes the absolute value
322 (Schaum et al., 2013). We then calculated the expected growth rate, POC quota and
323 PIC quota in LNLP conditions based on the measured trait values in HNHP

conditions and the change ratios in LNHP and HNLP conditions according to a linear model: $E_{LNLP} = (1 - R_{LNHP} - R_{HNLP}) \times M_{HNHP}$ for growth rate and POC quota; $E_{LNLP} = (1+R_{LNHP}+R_{HNLP}) \times M_{HNHP}$ for PIC quota (Brennan and Collins, 2015). We tested the significant differences between the expected trait values (E_{LNLP}) and the measured trait values (M_{LNLP}) in LNLP conditions by a one-way ANOVA (Fig. S3). We also calculated the extent of synergy between LNHP and HNLP on growth rate, POC quota and PIC quota according to equation: $S = | E_{LNLP} - M_{HNHP} | / M_{HNHP}$. Please see the discussion section for more information.

3 Results

3.1 Carbonate chemistry parameters and nutrient concentrations

During the incubations, pH_T values increased due to organismal activity by, on average, 0.03 ± 0.01 in LCLT, by 0.01 ± 0.01 in HCLT, by 0.02 ± 0.01 in LCHT and by 0.02 ± 0.01 in HCHT conditions (Fig. 1f–j; Table 1). Correspondingly, seawater pCO_2 concentrations decreased by 8.8% ± 1.1% in LCLT, by 6.1% ± 4.4% in HCLT, by 6.6% ± 1.7% in LCHT, and by 5.4% ± 3.6% in HCHT conditions, respectively (Fig. 1k–o; Table 1).

During the incubations, dissolved inorganic nitrogen (DIN) concentrations decreased by 28.7% ± 6.7% in HNHP and LL (Fig. 1p), by 26.8% ± 5.9% in HNHP and HL (Fig. 1q), by 71.1% ± 3.3% in LNHP (Fig. 1r), by 32.9% ± 5.6% in HNLP (Fig. 1s), and by 69.8% ± 3.2% in LNLP conditions (Fig. 1t; Table 2). Dissolved inorganic phosphate (DIP) concentrations decreased by 62.2% ± 16.5% in HNHP and LL (Fig. 1u), by 71.3% ± 6.7% in HNHP and HL (Fig. 1v), by 61.0% ± 5.2% in LNHP (Fig. 1w), by 83.8% ± 5.4% in HNLP (Fig. 1x), and by 86.3% ± 1.4% in LNLP conditions (Fig. 1y; Table 2).

349 Overall, while organismal activity affected nutrient levels during growth cycles as
350 expected, the high and low nutrient treatments remained different at all times (Table
351 2). Organismal activity had minimal effects on carbonate chemistry (see Fig. 1).
352

353 **3.2 Population growth rate**

354 Growth rate was significantly lower under the future scenario (HCHT HL LNLP: high
355 levels of pCO_2, temperature and light as well as low levels of nutrients) than under the
356 present scenario (LCLT LL HNHP: low levels of pCO_2, temperature and light
357 alongside high levels of nutrients) (one-way ANOVA, $F = 52.6$, $p < 0.01$) (Figs. 2a
358 and 3a,d; Table 2). The effect of increasing pCO_2 on growth rate is negative at low
359 light or low nutrients levels, which can be seen by comparing population growth in all
360 of the HC regimes with their paired LC regimes (Figs. 3a,b,e and S4). The extent of
361 reduction in population growth rate depends on which other stressors are present.
362 Compared to present atmospheric pCO_2 levels (LC, Fig. 3a), growth rates under ocean
363 acidification (HC, Fig. 3b) decreased by an average of 17.4% ± 1.3% in HNHP and
364 LL, and by an average of 4.4% ± 1.1% in HNHP and HL conditions (three-way
365 ANOVA, both $p < 0.01$; Tukey post hoc test, both $p < 0.01$) (Fig. 3e; Tables 2 and 3),
366 by 7.6% ± 2.6% in LNHP, by 21.4% ± 0.2% in HNLP, and by 32.1% ± 0.5% in
367 LNLP conditions under the HL, respectively (four-way ANOVA, all $p < 0.01$; Tukey
368 post hoc test, all $p < 0.01$) (Fig. 3a,b,e; Tables 2 and 4).

369 Across all HT/LT (high/low temperature) regime pairs, population growth rate is
370 faster in the HT regimes, indicating that increasing temperature from 16 to 20 ºC
371 increases population growth rate in *E. huxleyi* (Figs. 3a,c,f and S4). Compared to the
372 low temperature (LT, Fig. 3a), growth rates at the high temperature (HT, Fig. 3c)
373 increased by 7.7% ± 0.7% in HNHP and LL, and by 34.0% ± 0.4% in HNHP and HL

374 conditions (three-way ANOVA, both $p < 0.01$; Tukey post hoc test, both $p < 0.01$)
375 (Fig. 3a,c,f; Tables 2 and 3), by 42.4% ± 0.4% in LNHP, by 33.5% ± 0.5% in HNLP,
376 and by 40.4% ± 3.1% in LNLP conditions under HL (four-way ANOVA, all $p < 0.01$;
377 Tukey post hoc test, all $p < 0.01$) (Fig. 3a,c,f; Tables 2 and 4). Compared to low pCO_2
378 and low temperature (LCLT, Fig. 3a), growth rates in high pCO_2 and high
379 temperature environments (HCHT, Fig. 3d) increased by 3.9% ± 0.9% in HNHP and
380 LL, and by 31.1% ± 0.1% in HNHP and HL conditions (three-way ANOVA, both $p <$
381 0.01; Tukey post hoc test, both $p < 0.01$) (Fig. 3a,d,g; Tables 2 and 3), by 38.6% ±
382 0.1% in LNHP and by 17.1% ± 1.7% in HNLP, whereas growth rate decreased by
383 12.1% ± 2.2% in LNLP conditions under HL, respectively (four-way ANOVA, all $p <$
384 0.01; Tukey post hoc test, all $p < 0.01$) (Fig. 3a,d,g; Tables 2 and 4). These results
385 show that high pCO_2, low nitrate and low phosphate concentrations collectively
386 reduced the population growth rate in *E. huxleyi*, though elevated temperature could
387 counteract this response.

388 The effects of reduced availability of nutrients on growth are nutrient-specific (Fig.
389 3). Compared to HNHP and HL, growth rates in LNHP decreased by 3.0–12.1% (all p
390 < 0.05 at LCLT, HCLT, LCHT and HCHT conditions) (Fig. 3h; Tables 2 and 4). In
391 contrast, HNLP did not significantly affect growth in LC conditions ($p > 0.1$ in LCLT
392 and LCHT conditions) (Fig. 3a,c,i), but did lower population growth rate by 11.3–
393 19.2% in HC conditions (both $p < 0.01$ at HCLT and HCHT conditions) (Fig. 3b,d,i).
394 Unsurprisingly, when both nitrate and phosphate levels were reduced, growth rates
395 always decreased by larger extent compared to environments where they were
396 reduced individually (Fig. 3h,i,j). Compared to growth rates in HNHP and HL, growth
397 rates in LNLP were 4.8–10.2% lower in LC environments, and 34.7–40.3% lower in
398 HC environments (Tukey post hoc test, all $p < 0.01$ at LCLT, HCLT, LCHT and

399 HCHT conditions) (Fig. 3a–d,j; Tables 2 and 4). In summary, nitrate and phosphate
400 limitation exacerbated the impacts of OA and warming on population growth rate.
401

402 **3.3 POC quota**

403 Cellular POC quotas were two-fold larger under the future scenario (HCHT HL LNLP)
404 than under the current scenario (LCLT LL HNHP) (one-way ANOVA, F = 96.1, $p <$
405 0.01, Figs. 2b and 4a,d). The effect of increasing pCO_2 on POC quota is positive,
406 regardless of other drivers present, which can be seen by comparing POC quotas in all
407 of the HC regimes with their paired LC regimes (Figs. 4a,b,e and S4), though the
408 extent of increase in POC quota depends on which other stressors are present.
409 Compared to current atmospheric pCO_2 level (LC, Fig. 4a), POC quotas under ocean
410 acidification (Fig. 4b) increased by 40.3% ± 10.1% in HNHP and LL (Tukey post hoc
411 test, $p < 0.01$), by 13.8% ± 10.1% in HNHP and HL ($p = 0.47$), by 33.2% ± 11.1% at
412 LNHP, by 109.4% ± 14.0% in HNLP and by 87.3% ± 10.8% in LNLP conditions
413 under HL, respectively (four-way ANOVA, all $p < 0.01$; Tukey post hoc test, all $p <$
414 0.01) (Fig. 4a,b,e; Tables 2 and 4).

415 The effect of elevated temperature on POC quota can be seen by comparing POC
416 quota in all of the HT regimes with their paired LT regimes (Figs. 4a,c,f and S4).
417 Across all HT/LT regime pairs, POC quotas did not show significant differences
418 between the HT and LT regimes under HNHP and LL, HNHP and HL, LNHP, HNLP
419 and LNLP conditions under HL, respectively (Tukey post hoc test, all $p > 0.1$) (Fig.
420 4a,c,f). This demonstrated that increasing temperature within the test range had no
421 significant effect on POC quota. The combined effects of increasing pCO_2 and
422 temperature on POC quotas were nutrient dependent. Compared to low pCO_2 and low
423 temperature (LCLT, Fig. 4a), POC quotas at high pCO_2 and high temperature (HCHT,

424 Fig. 4d) did not show significant differences in HNHP and LL (p = 0.79), in HNHP
425 and HL (p = 0.99), and in LNHP and HL (p = 0.99), but increased by 52.2% ± 20.6%
426 in HNLP and by 45.6% ± 14.8% in LNLP conditions under HL (Tukey post hoc test,
427 both $p < 0.01$) (Fig. 4a,d,g; Tables 2 and 4). These data showed that high pCO_2 and
428 low phosphate concentrations enhanced POC quotas of *E. huxleyi*, and that their
429 combined effects were partly reduced by rising temperature.

430 The effects of nutrient reduction on POC quota are nutrient specific (Fig. 4).
431 Compared to HNHP and HL, POC quotas in LNHP did not show a significant
432 difference (all $p > 0.1$ at LCLT, HCLT, LCHT and HCHT) (Fig. 4a–d,h; Tables 2 and
433 4). At LC, POC quotas did not significantly differ between HNHP, HNLP and LNLP
434 conditions (Tukey post hoc test, all $p > 0.1$) (Fig. 4a,c,i,j). In contrast, in HC, they
435 were 43.3–78.2% larger in HNLP or LNLP than in HNHP (all $p < 0.01$) (Fig. 4b,d,i,j;
436 Table 2).

437

438 **3.4 PIC quota**

439 Cellular PIC quotas were significantly larger in the future scenario with high levels of
440 pCO_2, temperature and light along with low nutrients concentrations, than PIC quotas
441 in the present scenario with low levels of pCO_2, temperature and light along with
442 relatively high nutrients concentrations (one-way ANOVA, F = 63.6, $p < 0.01$) (Figs.
443 2c and 5a,d). However, the opposite results were found under the elevated CO_2
444 treatment alone. The effect of increasing pCO_2 on PIC quota is negative, regardless of
445 presence of other drivers. By comparing PIC quota in all of the HC regimes with their
446 paired LC regimes (Figs. 5a,b,e and S4), the effects of elevated pCO_2 level are clear,
447 though the extent of reduction in PIC quota depends on which other stressors are
448 present. Compared to present atmospheric pCO_2 levels (LC, Fig. 5a), PIC quotas

under ocean acidification (Fig. 5b) are reduced by 31.8% ± 17.1% in HNHP and LL, by 34.3% ± 10.0% in HNHP and HL, by 25.0% ± 3.8% in LNHP, by 22.8% ± 6.3% in HNLP and by 44.6% ± 0.9% in LNLP conditions under HL, respectively (Tukey post hoc test, all $p < 0.05$) (Fig. 5a,b,e; Tables 2–4). The extent of reduction in PIC quota is larger under LNLP conditions.

The effects of rising temperature on PIC quota were nutrient dependent, and can be seen by comparing PIC quotas in the HT regimes with those in their paired LT regimes (Figs. 5a,c,f and S4). Compared to low temperature (LT, Fig. 5a), PIC quotas at high temperature (HT, Fig. 5c) did not show significant differences in HNHP and LL, in HNHP and HL, in LNHP, and in HNLP conditions (Tukey post hoc test, all $p > 0.05$), whereas they decreased by 27.9% ± 8.4% in LNLP conditions under HL (Tukey post hoc test, $p < 0.01$) (Fig. 5a,c,f; Tables 2–4). The combined effects of rising pCO_2 and temperature on PIC quota are negative, regardless of which other drivers are present (Fig. 5a,d,g). Compared to low pCO_2 and low temperature (LCLT, Fig. 5a), PIC quotas in high pCO_2 and high temperature (HCHT, Fig. 5d) declined by 11.1% ± 10.9% in HNHP and LL ($p = 0.96$), by 32.5% ± 2.4% in HNHP and HL ($p < 0.01$), by 42.2% ± 3.2% in LNHP ($p < 0.01$), by 10.2% ± 7.7% in HNLP ($p = 0.92$), and by 45.3% ± 5.9% in LNLP conditions under HL, respectively ($p < 0.01$) (Fig. 5a,d,g; Table 2).

Effects of both nitrate and phosphate reduction on PIC quota are positive, regardless of levels of pCO_2 and temperature for the range used here (Fig. 5h,i,j). Compared to HNHP and HL, PIC quotas were larger in LNHP (Tukey post hoc test, $p < 0.01$ in LCLT, HCLT and LCHT conditions; $p = 0.73$ at HCHT condition) (Fig. 5h), in HNLP, and in LNLP conditions, respectively (all $p < 0.01$ at LCLT, HCLT, LCHT and HCHT conditions) (Fig. 5a–d,i,j; Table 2). In addition, PIC quotas were larger in

474 LNLP than in HNLP conditions (Tukey post hoc test, $p < 0.01$ in LCLT and HCLT
475 conditions; $p = 0.06$ in LCHT; $p = 0.21$ in HCHT conditions) (Fig. 5a–d,i,j). These
476 data showed that low nitrate and phosphate concentrations act synergistically to
477 increase PIC quotas, which was moderated under the high pCO_2.
478
479 **3.5 PIC / POC value**
480 The ratio of PIC to POC (PIC / POC value) was not significantly different between
481 the future scenario (HCHT HL LNLP) and the current scenario (LCLT LL HNHP)
482 (one-way ANOVA, F = 0.3, $p = 0.60$) (Figs. 2d and 6a,d). The PIC / POC value
483 followed the same trend as for PIC quotas described above. The effect of increasing
484 pCO_2 on PIC / POC value was negative, regardless of which other drivers were
485 present (Figs. 6a,b,e and S4), but the extent of reduction in PIC / POC value depended
486 on presence of other drivers. Compared to current atmospheric pCO_2 levels (LC, Fig.
487 6a), PIC / POC values under ocean acidification (HC, Fig. 6b) decreased by 50.7% ±
488 18.2% in HNHP and LL, by 41.8% ± 15.4% in HNHP and HL, by 43.9% ± 5.8% in
489 LNHP, by 63.0% ± 4.2% in HNLP, and by 70.7% ± 2.0% in LNLP conditions under
490 HL, respectively (Tukey post hoc test, all $p < 0.05$) (Fig. 6a,b,e; Table 2).
491 The effect of rising temperature on PIC / POC value was nutrient dependant (Figs.
492 6a,c,f and S4). Compared to low temperature (LT, Fig. 6a), PIC / POC values at high
493 temperature (HT, Fig. 6c) did not show significant differences in HNHP and LL, in
494 HNHP and HL, in LNHP, and in LNLP conditions (Tukey post hoc test, all $p > 0.1$),
495 whereas they increased by 39.0% ± 8.9% in HNLP conditions (Tukey post hoc test, p
496 $= 0.006$) (Fig. 6a,c,f; Table 2). The combined effects of elevated pCO_2 and
497 temperature on PIC / POC values were negative (Fig. 6a,d,g). Relative to low pCO_2
498 and low temperature (LCLT, Fig. 6a), PIC / POC values at high pCO_2 and high

temperature (HCHT, Fig. 6d) did not show significant differences in HNHP and LL, and in HNHP and HL conditions (Tukey post hoc test, both $p > 0.1$), but they decreased by 39.9% ± 3.0% in LNHP, by 40.6% ± 5.8% in HNLP, and by 67.8% ± 3.1% in LNLP conditions under HL, respectively (Tukey post hoc test, all $p < 0.01$) (Fig. 6a,d,g; Table 2).

Across all LNHP/HNHP (low/high nitrate) regime pairs, PIC / POC values were higher in the LNHP regime (Fig. 6h), though the extent of increase in PIC / POC values depended on pCO_2 or temperature levels. Compared to HNHP and HL, PIC / POC values in LNHP were about 106.0% ± 13.0% larger (Tukey post hoc test, $p < 0.05$ in LCLT and LCHT conditions; $p > 0.05$ in HCLT and HCHT conditions) (Fig. 6a–d, h; Table 2). The effect of phosphate on PIC / POC value also depended on pCO_2 levels (Fig. 6i). In LC, PIC / POC values were larger in HNLP than in HNHP ($p = 0.22$ at LCLT; $p < 0.05$ at LCHT conditions), and in LNLP than in LP ($p < 0.01$ at LCLT; $p = 0.09$ in LCHT conditions) (Fig. 6a,c). In HC conditions, PIC / POC values did not show significant differences among HNHP, HNLP and LNLP conditions (Tukey post hoc test, all $p > 0.05$ in HCLT and HCHT conditions) (Fig. 6b,d; Table 2).

4 Discussion

Understanding effects of multiple drivers is helpful for improving how coccolithorphores are represented in models (Krumhardt et al., 2017). Responses of growth, POC and PIC quotas to ocean acidification have been shown to be modulated by temperature (Gafar and Schulz, 2018; Tong et al., 2019), light intensity or light period (light : dark cycle) (Jin et al., 2017; Bretherton et al., 2019), DIN or DIP concentrations (Müller et al., 2017), combinations of light intensity and nutrients availability (Zhang et al., 2019) (Table 5). Following up our previous study (Zhang et

524 al., 2019), we added temperature as a key driver of 5 drivers (Table S2), and explored
525 how temperature changes would modulate the combined effects of CO_2, light, DIN
526 and DIP that we previously reported. Our data showed that a future ocean climate
527 change cluster (increasing CO_2, temperature, and light levels along with decreasing
528 DIN and DIP levels) can lower growth rate with increased POC and PIC quota per
529 cell (Fig. 2) as a result of plastic responses to the drivers. In contrast, observations of
530 coccolithophore Chl *a* increased from 1990 to 2014 in the North Atlantic, and rising
531 CO_2 and temperature has been aassociated with accelerated growth of
532 coccolithophores since 1965 in the North Atlantic (Rivero-Calle et al., 2015;
533 Krumhardt et al., 2016). Our results from laboratory experiments with multiple
534 drivers experiment instead predicted a different trend with progressive ocean climate
535 changes. We have to admit that results from laboratory experiments can hardly
536 extrapolate to natural conditions. Nevertheless, our data provide mechanistic
537 understanding of the combined effects of ocean climate change drivers, which can be
538 useful in analyzing field observations.

539 It should also be noted that regional responses to ocean global changes could differ
540 due to chemical and physical environmental differences and species and strain
541 variability among different oceans or regions (Blanco-Ameijeiras et al., 2016; Gao et
542 al., 2019), and that this could also explain discrepancies between experiments and
543 observations. Different *E. huxleyi* strains displayed optimal responses to a broad range
544 of temperature or CO_2 level, and *E. huxleyi* strains isolated from different regions
545 showed local adaptation to temperature or CO_2 level (Zhang et al., 2014; 2018).
546 Strain-specific responses of growth, POC and PIC production rates in *E. huxleyi*
547 isolated from different regions to changing seawater carbonate chemistry have also
548 been documented (Langer et al., 2009). It has been suggested that inter-strain genetic

549 variability has greater potential to induce larger phenotypic differences than the
550 phenotypic plasticity of a single strain cultured under a broad range of variable
551 environmental conditions (Blanco-Ameijeiras et al., 2016). On the other hand, the
552 genetic adaptation to culture experimental conditions over time may no longer
553 accurately represent the cells in the sea, as reflected in a diatom (Guan and Gao, 2008).
554 Phytoplankton species that had been maintained under laboratory conditions might
555 have lost original traits and display different responses to environmental changes
556 (Lakeman et al., 2009). The strain used in this study has been kept in the laboratory
557 for about 30 years, and the data obtained in this work can hardly reflect relation to its
558 biogeographic origin.

559 The decreased availability of nitrate or phosphate individually reduced growth rate
560 and increased PIC quota, respectively, in this experiment. Furthermore, under LNLP
561 and high pCO_2 levels, measured growth rates were significantly lower than the
562 expected values estimated on the basis of the values in LNHP and HNLP conditions
563 (Fig. S3a). This indicates synergistic negative effects of LN and LP on growth rate, an
564 evidence that colimitation of N and P is more severe than that by N or P alone. Here,
565 the extent of synergy between LN and LP on growth rate was calculated to be
566 8.6%±2.8% at low temperature and to be 40.6%±3.8% at high temperature (Fig. S3a),
567 suggesting modulating effect of temperature on response of growth rate to nutrient
568 limitations (Thomas et al., 2017). Similarly, at LNLP and low pCO_2 level, the
569 measured PIC quota was significantly larger than the expected value (Fig. S3c),
570 indicating synergistic positive effects of LN and LP on PIC quota, with the extent of
571 synergy being 31.4%±3.9% at low temperature. LN and LP did not synergistically act
572 to reduce POC quota.

While there were always interactions among stressors, increased temperature itself sped up population growth to a relatively consistent value at high light, regardless of nutrient limitation, with statistically significant but small differences over the different nutrient regimes (Fig. 3f). Rising pCO_2 level not only decreased the absolute values of growth rate, but also reduced the positive effect of high temperature on growth. In addition, elevated pCO_2 also altered patterns of growth responses to changes in light and nutrient levels (Fig. 3e–g). In ocean acidification condition, the negative effect of low pH on growth rate of the same *E. huxeyi* strain PML B92/11 was larger than the positive effect of high CO_2 concentration (Bach et al., 2011). Our data further showed that low-pH inhibited growth to lesser extent under the high light than under low light (Fig. 3e; Table 2). One possible explanation for this could be that photosynthesis under the high light regime could generate more energy-conserving compounds (Fernández et al., 1996). This results in faster pCO_2 removal and counteracts the negative effects of low pH. This interaction between low pH and high light was also observed when *E. huxleyi* strains PML B92/11 and CCMP 2090 were grown under incident sunlight (Jin et al., 2017).

Increases in temperature reduced PIC quotas under some conditions (high light (HL), HL-LNHP and HL-LNLP) (Fig. 5f), suggesting that the ratio of N:P is important in modulating calcification under warming. One striking result is the consistent negative effect of high pCO_2 on growth and PIC quota, regardless of other stressors. While pCO_2 levels affected the absolute PIC values, the combination of high pCO_2 and warming did not affect the responses to light and nutrients once the direct reduction in PIC quota due to increased pCO_2 was taken into account (Fig. 5g). It has been documented that PIC quotas of *E. huxleyi* strain PML B92/11 reduced at high pCO_2 due to suppressed calcification (Riebesell and Tortell, 2011). This

598 knowledge has been based on experiments under nutrient-replete or constant
599 conditions without consideration of multiple drivers. In this work, PIC quota of *E.*
600 *huxleyi* under OA were raised with increased light intensity and decreased availability
601 of nutrients (Figs. 2 and 5). These results are consistent with other studies (Perrin et
602 al., 2016; Jin et al., 2017), which reported that nutrient limitations enhanced
603 calcification, and high light intensity could make cells to remove H^+ faster and then
604 reduce the negative effect of low pH on calcification of *E. huxleyi* (Jin et al., 2017).
605 Our data also indicate that effects of ocean climate change on calcification of *E.*
606 *huxleyi* are more complex than previously thought (Meyer and Riebesell, 2015). It is
607 worth noting that the observed higher POC and PIC quotas under future ocean climate
608 change scenario could be attributed to cell cycle arrest of a portion of the community
609 (Vaulot et al., 1987). Decreased availabilities of nitrate and phosphate can extend the
610 G1 phase where photosynthetic carbon fixation and calcification occurred, and lead to
611 lower dark respiration which reduces carbon consumption (Vaulot et al., 1987; Müller
612 et al., 2008; Gao et al., 2018).

613 Synthesis of RNA is a large biochemical sink for phosphate in *E. huxleyi* and other
614 primary producers (Dyhrman, 2016). In this study, RNA content per cell was verified
615 by a SYBR Green method (Berdalet et al., 2005). Compared to HNHP conditions,
616 HNLP-grown cells had only 7.8% of total RNA (Fig. S11). This indicates that
617 decreased availability of phosphate strongly decreased RNA synthesis, which would
618 consequently extend the interphase of the cell cycle where calcification occurs
619 (Müller et al., 2008). This could explain why PIC quotas were enhanced by decreased
620 phosphate availability (Fig. 5). Similarly, decreased availability of nitrate decreased
621 protein (or PON) synthesis (Fig. S10), which can also block cells in the interphase of
622 the cell cycle, and increase the time available for calcification in *E. huxleyi* (Vaulot et

623 al., 1987). Consistently with this, lower rates of assimilation or organic matter
624 production in *E. huxleyi* in LNHP than in HNHP treatments are consistent with more
625 energy being reallocated to use for calcification (Nimer and Merrett, 1993; Xu and
626 Gao, 2012).

627 Low phosphate concentrations can induce high affinity phosphate uptake in *E.*
628 *huxleyi* (Riegman et al., 2000; Dyhrman and Palenik, 2003; McKew et al., 2015). This
629 mechanism enables *E. huxleyi* to take up phosphate efficiently at low pCO_2
630 concentrations, so that no significant difference in growth rate was observed between
631 HNLP and HNHP treatments (Fig. 3a,c). However, at high pCO_2, low phosphate
632 concentration (HNLP) lowered growth of *E. huxleyi* relative to HNHP (Fig. 3a–d;
633 Table 2). While the affinity of *E. huxleyi* for phosphate under different pCO_2 levels
634 has not been studied, the extra energetic cost of coping with stress from high pCO_2
635 could limit the energy available for the active uptake of phosphate. In addition, the
636 activity of alkaline phosphatase, which might work to reuse released organic P,
637 decreases at low pH (Rouco et al., 2013). Finally, the enlarged cell volume in HC and
638 HNLP (or LNLP) conditions may further reduce nutrient uptake by cells due to
639 reduced surface to volume ratios, and lower cell division rates (Fig. S5) (Finkel, 2001).
640 While substantial evolutionary responses to multiple drivers may help further, our
641 results imply that decreased phosphate availability along with progressive ocean
642 acidification and warming in surface ocean may reduce the competitive capability of
643 *E. huxleyi* in oligotrophic waters. Meanwhile, HNLP also affected expressions of
644 genes related to nitrogen metabolism due to the tight stoichiometric coupling of
645 nitrogen and phosphate metabolism (Rokitta et al., 2016). Decreased availability of
646 nitrate further limited nitrogen metabolism of *E. huxleyi* (Rokitta et al., 2014), which
647 lowered the overall biosynthetic activity and reduced cellular PON quotas (Fig. S10).

648 These explain the synergistic inhibitions of low-pH, low-phosphate and low-nitrate on
649 growth of *E. huxleyi* (Fig. 3).

650 POC quotas and the cell-volume normalized POC quotas were larger at high pCO_2
651 than at low pCO_2 under all treatments (Figs. 4; S6; Table 2), which could be a
652 combined outcome of increased photosynthetic carbon fixation (Zondervan et al.,
653 2002; Hoppe et al., 2011; Tong et al., 2019) and reduced cell division (present work),
654 leading to pronounced increase of POC quotas in the cells grown under low phosphate
655 (HNLP) and high pCO_2 (Fig. 4). At HNLP and high pCO_2 levels, photosynthetic
656 carbon fixation proceeds whereas cell division rate decreases (Figs. 3 and 4), so
657 reallocation of newly produced particulate organic carbon (POC) could be slowed
658 down (Vaulot et al., 1987). In this case, over-synthesis of cellular organic carbon
659 might be released as dissolved organic carbon (DOC), which can coagulate to
660 transparent exopolymer particles (TEP) and attach to cells (Biermann and Engel, 2010;
661 Engel et al., 2015). When cells were filtered on GF/F filters, any TEP would not have
662 be separated from the cells and would have contributed to the measured POC quota in
663 this study.

664 Large PIC quotas of coccolithophores may facilitate accumulation of calcium
665 carbonate in the deep ocean and increase the contribution of $CaCO_3$ produced by
666 coccolithophores to calcareous ooze in the pelagic ocean (Hay, 2004). Due to $CaCO_3$
667 being more dense than organic carbon, larger PIC quotas may facilitate effective
668 transport of POC to deep oceans, leading to vertical DIC or CO_2 gradients of seawater
669 (Milliman, 1993; Ziveri et al., 2007). While the effects of global ocean climate
670 changes on physiological processes of phytoplankton can be complex, our results
671 promote our understanding on how a cosmopolitan coccolithophore responds to future
672 ocean environmental changes through plastic trait change.

Data availability. The data are available upon request to the corresponding author (Kunshan Gao).

Author contributions. YZ, KG designed the experiment. YZ performed this experiment. All authors analysed the data, wrote and improved the manuscript.

Competing interests. The authors declare that they have no conflict of interest.

Acknowledgements. This study was supported by National Natural Science Foundation of China (41720104005, 41806129, 41721005), and Joint Project of National Natural Science Foundation of China and Shandong province (No. U1606404).

References

Bach, L. T., Riebesell, U., and Schulz, K. G.: Distinguishing between the effects of ocean acidification and ocean carbonation in the coccolithophore *Emiliania huxleyi*, Limnol. Oceanogr., 56, 2040–2050, doi: 10.4319/lo.2011.56.6.2040, 2011.

Barton, A. D., Irwin, A. J., Finkel, Z. V., and Stock, C. A.: Anthropogenic climate change drives shift and shuffle in North Atlantic phytoplankton communities, Proc. Nat. Aca. Sci. USA, 113, 2964–2969, doi:10.1073/pnas.1519080113, 2016.

Berdalet, E., Roldán, C., Olivar, M. P., and Lysnes, K.: Quantifying RNA and DNA in planktonic organisms with SYBR Green II and nucleases. Part A. Optimisation of the assay, Sci. Mar., 69, 1–16, doi: 10.3989/scimar.2005.69n11, 2005.

Biermann, A., and Engel, A.: Effect of CO_2 on the properties and sinking velocity of aggregates of the coccolithophore *Emiliania huxleyi*, Biogeosciences, 7, 1017–1029, doi :10.5194/bg-7-1017-2010, 2010.

Blanco-Ameijeiras, S., Lebrato, M., Stoll, H. M., Iglesias-Rodriguez, D., Müller, M. N., Méndez-Vicente, A., and Oschlies, A.: Phenotypic variability in the coccolithophore *Emiliania huxleyi*, Plos ONE, 11, e0157697, doi: 10.1371/journal.pone.0157697, 2016.

Borchard, C., Borges, A. V., Händel, N., and Engel, A.: Biogeochemical response of *Emiliania huxleyi* (PML B92/11) to elevated CO_2 and temperature under phosphorus limitation: A chemostat study, J. Exp. Mar. Biol. Ecol., 410, 61–71, doi: 10.1016/j.jembe.2011.10.004, 2011.

Boyd, P. W., Collins, S., Dupont, S., Fabricius, K., Gattuso, J. P., Havenhand, J., Hutchins, D. A., Riebesell, U., Rintoul, M. S., Vichi, M., Biswas, H., Ciotti, A.,

Gao, K., Gehlen, M., Hurd, C. L., Kurihara, H., McGraw, C. M., Navarro, J. M., Nilsson, G. E., Passow, U., and Pörtner, H. O.: Experimental strategies to assess the biological ramifications of multiple drivers of global ocean change—A review, Global Change Biol., 24, 2239–2261, doi: 10.1111/gcb.14102, 2018.

Boyd, P. W., Dillingham, P. W., McGraw, C. M., Armstrong, E. A., Cornwall, C. E., Feng, Y., Hurd, C. L., Gault-Ringold, M., Roleda, M. Y., Timmins-Schiffman, E., and Nunn, B. L.: Physiological responses of a Southern Ocean diatom to complex future ocean conditions, Nat. Clim. Change, 6, 207–213, doi: 10.1038/NCLIMATE2811, 2016.

Boyd, P. W., Lennartz, S. T., Glover, D. M., and Doney, S. C.: Biological ramifications of climate-change-mediated oceanic multi-stressors, Nat. Clim. Change, 5, 71–79, doi: 10.1038/nclimate2441, 2015.

Boyd, P. W., Strzepek, R., Fu, F., and Hutchins, D. A.: Environmental control of open-ocean phytoplankton groups: Now and in the future, Limnol. Oceanogr., 55, 1353–1376, doi: 10.4319/lo.2010.55.3.1353, 2010.

Brennan, G., and Collins, S.: Growth responses of a green alga to multiple environmental drivers, Nat. Clim. Change, 5, 892–897, doi: 10.1038/nclimate2682, 2015.

Brennan, G., Colegrave, N., and Collins, S.: Evolutionary consequences of multidriver environmental change in an aquatic primary producer, Proc. Nat. Aca. Sci. USA, 114, 9930–9935, doi: 10.1073/pnas.1703375114, 2017.

Bretherton, L., Poulton, A. J., Lawson, T., Rukminasari, N., Balestreri, C., Schroeder, D., Mark Moore, C., and Suggett, D. J.: Day length as a key factor moderating the response of coccolithophore growth to elevated pCO_2, Limnol. Oceanogr., 64, 1284–1296, doi: 10.1002/lno.11115, 2019.

De Bodt, C., Van Oostende, N., Harlay, J., Sabbe, K., and Chou, L.: Individual and interacting effects of pCO_2 and temperature on *Emiliania huxleyi* calcification: study of the calcite production, the coccolith morphology and the coccosphere size, Biogeosciences, 7, 1401–1412, doi: 10.5194/bg-7-1401-2010, 2010.

Dickson, A. G., Afghan, J. D., and Anderson, G. C.: Reference materials for oceanic CO_2 analysis: a method for the certification of total alkalinity, Mar. Chem., 80, 185–197, doi: 10.1016/S0304-4203(02)00133-0, 2003.

Dyhrman, S. T., and Palenik, B.: Characterization of ectoenzyme activity and phosphate-regulated proteins in the coccolithophorid *Emiliania huxleyi*, J. Plankton Res., 25, 1215–1225, doi: 10.1093/plankt/fbg086, 2003.

Dyhrman, S. T.: Nutrients and their acquisition: phosphorus physiology in microalgae, in: The physiology of microalgae, edited by: Borowitzka, M. A., Beardall, J. and Raven, J. A., Springer, Heidelberg, 155–183, doi: 10.1007/978-3-319-24945-2, 2016.

Engel, A., Borchard, C., Loginova, A. N., Meyer, J., Hauss, H., and Kiko, R.: Effects of varied nitrate and phosphate supply on polysaccharidic and proteinaceous gel particles production during tropical phytoplankton bloom experiments, Biogeosciences, 12, 5647–5665, doi: 10.5194/bg-12-5647-2015, 2015.

Feng, Y., Roleda, M. Y., Armstrong, E., Boyd, P. W., and Hurd., C. L.: Environmental controls on the growth, photosynthetic and calcification rates of a southern hemisphere strain of the coccolithophore *Emiliania huxleyi*, Limnol. Oceanogr., 62, 519–540, doi: 10.1002/lno.10442, 2017.

Feng, Y., Warner, M. E., Zhang, Y., Sun, J., Fu, F., Rose, J. M., and Hutchins, D. A.: Interactive effects of increased pCO_2, temperature and irradiance on the marine

coccolithophore *Emiliania huxleyi* (Prymnesiophyceae), Eur. J. Phycol., 43, 87–98, doi: 10.1080/09670260701664674, 2008.

Fernández, E., Fritz, J. J., and Balch, W. M.: Chemical composition of the coccolithophorid *Emiliania huxleyi* under light-limited steady state growth. J. Exp. Mar. Biol. Ecol., 207, 149–160. doi: 10.1016/S0022-0981(96)02657-3, 1996.

Finkel, Z. V.: Light absorption and size scaling of light-limited metabolism in marine diatoms, Limnol. Oceanogr., 46, 86–94, doi: 10.4319/lo.2001.46.1.0086, 2001.

Gafar, N. A., and Schulz, K. G.: A three-dimensional niche comparison of *Emiliania huxelyi* and *Gephyrocapsa oceanica*: reconciling observations with projections, Biogeosciences, 15, 3541–3560, doi: 10.5194/bg-15-3541-2018, 2018.

Gao, G., Xia, J., Yu, J., and Zeng, X.: Physiological response of a red tide alga (*Skeletonema costatum*) to nitrate enrichment, with special reference to inorganic carbon acquisition, Mar. Environ. Res., 133, 15–23, doi: 10.1016/j.marenvres.2017.11.003, 2018.

Gao, K., Beardall, J., Häder, D. P., Hall-Spencer, J. M., Gao, G., and Hutchins, D. A.: Effects of ocean acidification on marine photosynthetic organisms under the concurrent influences of warming, UV radiation, and deoxygenation, Front. Mar. Sci., 6, 322, doi: 10.3389/fmars.2019.00322, 2019.

Gao, K., Ruan, Z., Villafañe, V. E., Gattuso, J., and Walter-Helbling, E.: Ocean acidification exacerbates the effect of UV radiation on the calcifying phytoplankton *Emiliania huxleyi*, Limnol. Oceanogr., 54, 1855–1862, doi: 10.4319/lo.2009.54.6.1855, 2009.

Guan, W., and Gao, K.: Light histories influence the impacts of solar ultraviolet radiation on photosynthesis and growth in a marine diatom, *Skeletonema*

costatum, J. Photoch. Photobio. B., 91, 151–156, doi: 10.1016/j.jphotobiol.2008.03.004, 2008.

Hansen, H. P., and Koroleff, F.: Determination of nutrients, in: Methods of seawater analysis, edited by: Grasshoff, K., Kremling, K. and Ehrhardt, M., WILEY-VCH Publishers, ISBN: 3-527-29589-5, 1999.

Hay, W. W.: Carbonate fluxes and calcareous nannoplankton, in: Coccolithophores: from molecular biology to global impact, edited by: Thierstein, H. R. and Young, J. R., Springer, Berlin, 509–528, 2004.

Hoppe, C. J. M., Langer, G., and Rost, B.: *Emiliania huxleyi* shows identical responses to elevated pCO_2 in TA and DIC manipulations, J. Exp. Mar. Biol. Ecol., 406, 54–62, doi: 10.1016/j.jembe.2011.06.008, 2011.

Jin, P., Ding, J. C., Xing, T., Riebesell, U., and Gao, K. S.: High levels of solar radiation offset impacts of ocean acidification on calcifying and non-calcifying strains of *Emiliania huxleyi*, Mar. Ecol. Prog. Ser., 568, 47–58, doi: 10.3354/meps12042, 2017.

Kottmeier, D. M., Rokitta, S. D., and Rost, B.: Acidification, not carbonation, is the major regulator of carbon fluxes in the coccolithophore *Emiliania huxleyi*, New Phytol., 211, 126–137, doi: 10.1111/nph.13885, 2016.

Krumhardt, K. M., Lovenduski, N. S., Iglesias-Rodriguez, M. D., and Kleypas, J. A.: Coccolithophore growth and calcification in a changing ocean, Prog. Oceanogr., 171, 276–295, doi: 10.1016/j.pocean.2017.10.007, 2017.

Krumhardt, K. M., Lovenduski, N. S., Freeman, N. M., and Bates, N. R.: Apparent increase in coccolithophore abundance in the subtropical North Atlantic from 1990 to 2014, Biogeosciences, 13, 1163–1177, doi: 10.5194/bg-13-1163-2016, 2016.

Kwiatkowski, L., Aumont, O., and Bopp, L.: Consistent trophic amplification of marine biomass declines under climate change, Glob. Change Biol., 25, 218–229, doi: 10.1111/gcb.14468, 2019.

Lakeman, M. B., von Dassow, P., and Cattolico, R. A.: The strain concept in phytoplankton ecology, Harmful Algae, 8, 746–758, doi: 10.1016/j.hal.2008.11.011, 2009.

Langer, G., Nehrke, G., Probert, I., Ly, J., and Ziveri, P.: Strain-specific responses of *Emiliania huxleyi* to changing seawater carbonate chemistry, Biogeosciences, 6, 2637–2646, doi: 10.5194/bg-6-2637-2009.

Larsen, A., Flaten, G. A. F., Sandaa, R., Castberg, T., Thyrhaug, R., Erga, S. R., Jacquet, S., and Bratbak, G.: Spring phytoplankton bloom dynamics in Norwegian coastal waters: Microbial community succession and diversity, Limnol. Oceanogr., 49, 180–190, doi: 10.4319/lo.2004.49.1.0180, 2004.

Leonardos, N., and Geider, R. J.: Elevated atmospheric carbon dioxide increases organic carbon fixation by *Emilinia huxleyi* (haptophyta), under nutrient-limited high-light conditions, J. Phycol., 41, 1196–1203, doi: 10.1111/j.1529-8817.2005.00152.x, 2005.

Li, W., Yang, Y., Li, Z., Xu, J., and Gao, K.: Effects of seawater acidification on the growth rates of the diatom *Thalassiosira (Conticribra) weissflogii* under different nutrient, light and UV radiation regimes, J. Appl. Phycol., 29, 133–142, doi: 10.1007/s10811-016-0944-y, 2017.

Locarnini, R. A., Mishonov, A. V., Antonov, J. I., Boyer, T. P., and Garcia, H. E.: World ocean atlas 2005, V. 1: Temperature, edited by: Levitus, S., NOAA Atlas NESDIS 61. U. S. Government Printing Office, 123–134, 2006.

Matthiessen, B., Eggers, S. L., and Krug, S. A.: High nitrate to phosphorus regime attenuates negative effects of rising pCO_2 on total population carbon accumulation, Biogeosciences, 9, 1195– 1203, doi: 10.5194/bg-9-1195-2012, 2012.

McKew, B. A., Metodieva, G., Raines, C. A., Metodiev, M. V., and Geider, R. J.: Acclimation of *Emiliania huxleyi* (1516) to nutrient limitation involves precise modification of the proteome to scavenge alternative sources of N and P, Environ. Microbiol., 17, 1–13, doi: 10.1111/1462-2920.12957, 2015.

Meyer, J., and Riebesell, U.: Reviews and syntheses: response of coccolithophores to ocean acidification: a meta-analysis, Biogeosciences, 12, 1671–1682, doi: 10.5194/bg-12-1671-2015, 2015.

Milliman, J. D.: Production and accumulation of calcium carbonate in the ocean: budget of a nonsteady state, Global Biogeochem. Cy., 7, 927–957, doi: 10.1029/93GB02524, 1993.

Monteiro, F. M., Bach, L. T., Brownlee, C., Bown, P., Rickaby, R. E. M., Poulton, A. J., Tyrrell, T., Beaufort, L., Dutkiewicz, S., Gibbs, S., Gutowska, M. A., Lee, R., Riebesell, U., Young, J., and Ridgwell, A.: Why marine phytoplankton calcify, Sci. Adv., 2, 1–14, doi: 10.1126/sciadv.1501822, 2016.

Müller, M. N., Antia, A. N., and LaRoche, J.: Influence of cell cycle phase on calcification in the coccolithophore *Emiliania huxleyi*, Limnol. Oceanogr., 53, 506–512, doi: 10.4319/lo.2008.53.2.0506, 2008.

Müller, M. N., Beaufort, L., Bernard, O., Pedrotti, M. L., Talec, A., and Sciandra, A.: Influence of CO_2 and nitrogen limitation on the coccolith volume of *Emiliania huxleyi* (Haptophyta), Biogeosciences, 9, 4155–4167, doi: 10.5194/bg-9-4155-2012, 2012.

Müller, M. N., Trull, T. W., and Hallegraeff, G. M.: Independence of nutrient limitation and carbon dioxide impacts on the Southern Ocean coccolithophore *Emiliania huxleyi*, The ISME J., 11, 1777–1787, doi: 10.1038/ismej.2017.53, 2017.

Nimer, N. A., and Merrett, M. J.: Calcification rate in *Emiliania huxleyi* Lohmann in response to light, nitrate and availability of inorganic carbon, New Phytol., 123, 673–677, doi: 10.1111/j.1469-8137.1993.tb03776.x, 1993.

Omar, A. M., Olsen, A., Johannessen, T., Hoppema, M., Thomas, H., and Borges, A. V.: Spatiotemporal variations of fCO_2 in the North Sea, Ocean Sci., 6, 77–89, doi: 10.5194/osd-6-1655-2009, 2010.

Perrin, L., Probert, I., Langer, G., and Aloisi, G.: Growth of the coccolithophore *Emiliania huxleyi* in light- and nutrient-limited batch reactors: relevance for the BIOSOPE deep ecological niche of coccolithophores, Biogeosciences, 13, 5983–6001, doi: 10.5194/bg-13-5983-2016, 2016.

Pierrot, D., Lewis, E., and Wallace, D. W. R.: MS Excel program developed for CO_2 system calculations, ORNL/CDIAC-105, Carbon Dioxide Information Analysis Centre, Oak Ridge National Laboratory, U.S., Department of Energy, doi: 10.3334/CDIAC/otg.CO2SYS_XLS_CDIAC105a, 2006.

R version 3.5.0.: The R foundation for statistical computing platform: x86_64-w64-mingw32/x64, 2018.

Riebesell, U., and Gattuso, J. P.: Lessons learned from ocean acidification research, Nat. Clim. Change, 5, 12–14, doi: 10.1038/nclimate2456, 2015.

Riebesell, U., and Tortell, P. D.: Effects of ocean acidification on pelagic organisms and ecosystems, in: Ocean acidification, edited by: Gattuso, J. P. and Hansson, L., Oxford University Press, 99–121, 2011.

Riegman, R., Stolte, W., Noordeloos, A. A. M., and Slezak, D.: Nutrient uptake and alkaline phosphatase (EC 3:1:3:1) activity of *Emiliania huxleyi* (Prymnesiophyceae) during growth under N and P limitation in continuous cultures, J. Phycol., 36, 87–96, doi: 10.1046/j.1529-8817.2000.99023.x, 2000.

Rivero-Calle, S., Gnanadesikan, A., Del Castillo, C. E., Balch, W. M., and Guikema, S. D.: Multidecadal increase in North Atlantic coccolithophores and the potential role of rising CO_2, Science, 350, 1533–1537, doi: 10.1126/science.aaa8026, 2015.

Rokitta, S. D., von Dassow, P., Rost, B., and John, U.: *Emiliania huxleyi* endures N-limitation with an efficient metabolic budgeting and effective ATP synthesis, BMC Genomics, 15, 1051–1064, doi: 10.1186/1471-2164-15-1051, 2014.

Rokitta, S. D., von Dassow, P., Rost, B., and John, U.: P- and N-depletion trigger similar cellular responses to promote senescence in eukaryotic phytoplankton, Front. Mar. Sci., 3, 109, doi: 10.3389/fmars.2016.00109, 2016.

Rosas-Navarro, A., Langer, G., and Ziveri, P.: Temperature affects the morphology and calcification of *Emiliania huxleyi* strains, Biogeosciences, 13, 2913–2926, doi: 10.5194/bg-13-2913-2016, 2016.

Rost, B., and Riebesell, U.: Coccolithophores and the biological pump: responses to environmental changes, in: Coccolithophores : from molecular biology to global impact, edited by: Thierstein, H. R. and Young, J. R., Springer, Berlin, 99–125, 2004.

Rost, B., Zondervan, I., and Riebesell, U.: Light-dependent carbon isotope fractionation in the coccolithophorid *Emiliania huxleyi*, Limnol. Oceanogr., 47, 120–128, doi: 10.2307/3069125, 2002

Rouco, M., Branson, O., Lebrato, M., and Iglesias-Rodríguez, M.: The effect of nitrate and phosphate availability on *Emiliania huxleyi* (NZEH) physiology

921 under different CO_2 scenarios, Front. Microbiol., 4, 1–11, doi:
922 10.3389/fmicb.2013.00155, 2013.
923 Roy, R. N., Roy, L. N., Vogel, K. M., Porter-Moore, C., Pearson, T., Good, C. E.,
924 Millero, F. J., and Campbell, D. C.: Thermodynamics of the dissociation of boric
925 acid in seawater at S 5 35 from 0 degrees C to 55 degrees C, Mar. Chem., 44,
926 243–248, doi: 10.1016/0304-4203(93)90206-4, 1993.
927 Schaum, E., Rost, B., Millar, A. J., and Collins, S.: Variation in plastic responses of a
928 globally distributed picoplankton species to ocean acidification, Nat. Clim.
929 Change, 3, 298–302, doi: 10.1038/NCLIMATE1774, 2013.
930 Sett, S., Bach, L. T., Schulz, K. S., Koch-Klavsen, S., Lebrato, M., and Riebesell, U.:
931 Temperature modulates coccolithophorid sensitivity of growth, photosynthesis
932 and calcification to increasing seawater pCO_2, PLoS One, 9(2), e88308, doi:
933 10.1371/journal.pone.0088308, 2014.
934 Sunda, W. G., Price, N. M., and Morel, F. M. M.: Trace metal ion buffers and their
935 use in culture studies, in: Algal culturing techniques, edited by: Andersen, R. A.,
936 Elsevier Academic Press, 53–59, 2005.
937 Thomas, M. K., Aranguren-Gassis, M., Kremer, C. T., Gould, M. R., Anderson, K.,
938 Klausmeier, C. A., Litchman, E.: Temperature-nutrient interactions exacerbate
939 sensitivity to warming in phytoplankton, Global Change Biol., 23, 3269–3280,
940 doi: 10.1111/gcb.13641, 2017.
941 Tong, S., Hutchins, D., and Gao, K.: Physiological and biochemical responses of
942 *Emiliania huxleyi* to ocean acidification and warming are modulated by UV
943 radiation, Biogeosciences, 16, 561–572, doi: 10.5194/bg-16-561-2019, 2019.
944 Tong, S., Hutchins, D., Fu, F., and Gao, K.: Effects of varying growth irradiance and
945 nitrogen sources on calcification and physiological performance of the

946 coccolithophore *Gephyrocapsa oceanica* grown under nitrogen limitation,
947 Limnol. Oceanogr., 61, 2234–2242, doi: 10.1002/lno.10371, 2016.
948 Vaulot, D., Olson, R. J., Merkel, S., and Chisholm, S. E.: Cell-cycle response to
949 nutrient starvation in two phytoplankton species, *Thalassiosira weissflogii* and
950 *Hymenomonas carterae*, Mar. Biol., 95, 625–630, doi: 10.1007/BF00393106,
951 1987.
952 Xu, J., Gao, K., Li, Y., and Hutchins, D. A.: Physiological and biochemical responses
953 of diatoms to projected ocean changes, Mar. Ecol. Prog. Ser., 515, 73–81, doi:
954 10.3354/meps11026, 2014b.
955 Xu, K., Fu, F., and Hutchins, D. A.: Comparative responses of two dominant
956 Antarctic phytoplankton taxa to interactions between ocean acidification,
957 warming, irradiance, and iron availability, Limnol. Oceanogr., 59, 1919–1931,
958 doi: 10.4319/lo.2014.59.6.1919, 2014a.
959 Xu, K., and Gao, K.: Reduced calcification decreases photoprotective capability in the
960 coccolithophorid *Emiliania huxleyi*, Plant Cell Physiol., 53, 1267–1274, doi:
961 10.1093/pcp/pcs066, 2012.
962 Xu, K., Gao, K., Villafañe, V. E., and Helbling, E. W.: Photosynthetic responses of
963 *Emiliania huxleyi* to UV radiation and elevated temperature: roles of calcified
964 coccoliths, Biogeosciences, 8, 1441–1452, doi: 10.5194/bg-8-1441-2011, 2011.
965 Zhang, Y., Bach, L. T., Lohbeck, K. T., Schulz K. G., Listmann, L., Klapper R., and
966 Riebesell, U.: Population-specific responses in physiological rates of *Emilinia*
967 *huxleyi* to a broad CO_2 range, Biogeosciences, 15, 3691–3701, doi: 10.5194/bg-
968 15-3691-2018, 2018.

Zhang, Y., Fu, F., Hutchins, D. A., and Gao. K.: Combined effects of CO_2 level, light intensity and nutrient availability on the coccolithophore *Emiliania huxleyi*, Hydrobiologia, 842, 127–141, doi: 10.1007/s10750-019-04031-0, 2019.

Zhang, Y., Klapper, R., Lohbeck, K. T., Bach, L. T., Schulz, K. G., Reusch, T. B. H., and Riebesell, U.: Between- and within-population variations in thermal reaction norms of the coccolithophore *Emiliania huxleyi*, Limnol. Oceanogr., 59, 1570–1580, doi: 10.4319/lo.2014.59.5.1570, 2014.

Ziveri, P., deBernardi, B., Baumann, K., Stoll, H. M., and Mortyn, P. G.: Sinking of coccolith carbonate and potential contribution to organic carbon ballasting in the deep ocean, Deep Sea Res., 54, 659–675, doi: 10.1016/j.dsr2.2007.01.006, 2007.

Zondervan, I., Rost, B., and Riebesell, U.: Effect of CO_2 concentration on the PIC/POC ratio in the coccolithophore *Emiliania huxleyi* grown under light-limiting conditions and different daylengths, J. Exp. Mar. Biol. Ecol., 272, 55–70, doi: 10.1016/s0022-0981(02)00037-0, 2002.

994 **Figure Legends**

995 **Figure 1.** Four "baseline" environments were used where pCO_2 and temperature
996 (temp) were combined in all pairwise combinations: low pCO_2 + low temp (LCLT,
997 △), high pCO_2 + low temp (HCLT, ⋆), low pCO_2 + high temp (LCHT, □) and high
998 pCO_2 + high temp (HCHT, ○). Additional stressors were then added to each of the
999 four "baseline" environments. In step 1, low light (LL) was supplied. In step 2, high
1000 light (HL) was supplied. HL was then maintained for the rest of the experiment. In
1001 step 3, low nitrogen was supplied and high phosphate levels were restored (LNHP). In
1002 step 4, low phosphate was supplied and high nitrogen levels were restored (HNLP). In
1003 step 5, both nitrogen and phosphate were low (LNLP). Experimental steps were done
1004 in a consecutive manner. At each step, we measured cell concentration (**a**–**e**), medium
1005 pH_T value (**f**–**j**), medium pCO_2 level (**k**–**o**), dissolved inorganic nitrogen (DIN) (**p**–**t**)
1006 and phosphate (DIP) (**u**–**y**) concentrations in the media in the beginning and at the end
1007 of the incubations. Respectively, LC and HC represent pCO_2 levels of about 370 and
1008 960 μatm; LT and HT 16 and 20 °C; LL and HL 60 and 240 μmol photons m^{-2} s^{-1} of
1009 photosynthetically active radiation (PAR); HN and LN 24.3 and 7.8 μmol L^{-1} NO_3^- at
1010 the beginning of the incubation; HP and LP 1.5 and 0.5 μmol L^{-1} PO_4^{3-} at the
1011 beginning of the incubations. The samples were taken in the last day of the cultures in
1012 each treatment. The values were indicated as the means ± sd of 4 replicate populations
1013 for each treatment.

1014

1015 **Figure 2.** Growth rate (**a**), particulate organic (POC, **b**) and inorganic (PIC, **c**) carbon
1016 quotas, PIC / POC value (**d**) and cell volume (**e**) of *Emiliania huxleyi* grown under the
1017 present (defined as low levels of pCO_2, temperature and light along with high levels
1018 of nutrients) and the future (defined as higher levels of pCO_2, temperature, and light

1019 along with low levels of nutrients due to ocean acidification, warming and shoaling of
1020 upper mixing layer) scenarios. Data were obtained after cells were acclimated to
1021 experimental conditions for 14–16 generations and means ± sd of 4 replicate
1022 populations. Different letters (a, b) in each panel represent significant differences
1023 between future and present ocean conditions (Tukey Post hoc, $p < 0.05$).
1024
1025 **Figure 3.** Growth rates of *E. huxleyi* grown in LCLT (**a**), HCLT (**b**), LCHT (**c**) and
1026 HCHT (**d**) conditions, and the ratio of growth rate at HC to LC (**e**), HT to LT (**f**),
1027 HCHT to LCLT (**g**), LNHP to HNHP (**h**), HNLP to HNHP (**i**) and LNLP to HNHP (**j**).
1028 Data were obtained after cells were acclimated to experimental conditions for 14–16
1029 generations and means ± sd of 4 replicate populations. Horizontal lines in panels (**e**)–
1030 (**j**) showed the value of 1. Different letters (a, b, c, d) in panels (**a**)–(**d**) represent
1031 significant differences between different nutrient treatments (Tukey Post hoc, $p <$
1032 0.05). The results shown in the black column were used for the ambient-future
1033 comparison in figure 2. Detailed experimental conditions were shown in Figure 1.
1034
1035 **Figure 4.** POC quota of *E. huxleyi* grown in LCLT (**a**), HCLT (**b**), LCHT (**c**) and
1036 HCHT (**d**) conditions, and the ratio of POC quota at HC to LC (**e**), HT to LT (**f**),
1037 HCHT to LCLT (**g**), LNHP to HNHP (**h**), HNLP to HNHP (**i**) and LNLP to HNHP (**j**).
1038 Data were obtained after cells were acclimated to experimental conditions for 14–16
1039 generations and means ± sd of 4 replicate populations. Horizontal lines in panels (**e**)–
1040 (**j**) showed the value of 1. Different letters (a, b) in panels (**a**)–(**d**) represent significant
1041 differences between different nutrient treatments (Tukey Post hoc, $p < 0.05$). The
1042 results shown in the black column were used for the ambient-future comparison in
1043 figure 2. Detailed experimental conditions were shown in Figure 1.

1044

1045 **Figure 5.** PIC quota of *E. huxleyi* grown in LCLT (**a**), HCLT (**b**), LCHT (**c**) and
1046 HCHT (**d**) conditions, and the ratio of PIC quota at HC to LC (**e**), HT to LT (**f**),
1047 HCHT to LCLT (**g**), LNHP to HNHP (**h**), HNLP to HNHP (**i**) and LNLP to HNHP (**j**).
1048 Data were obtained after cells were acclimated to experimental conditions for 14–16
1049 generations and means ± sd of 4 replicate populations. Horizontal lines in panels (**e**)–
1050 (**j**) showed the value of 1. Different letters (a, b, c) in panels (**a**)–(**d**) represent
1051 significant differences between different nutrient treatments (Tukey Post hoc, $p <$
1052 0.05). The results shown in the black column were used for the ambient-future
1053 comparison in figure 2. Detailed experimental conditions were shown in Figure 1.

1054

1055 **Figure 6.** PIC / POC value of *E. huxleyi* grown in LCLT (**a**), HCLT (**b**), LCHT (**c**)
1056 and HCHT (**d**) conditions, and the ratio of (PIC / POC value) at HC to LC (**e**), HT to
1057 LT (**f**), HCHT to LCLT (**g**), LNHP to HNHP (**h**), HNLP to HNHP (**i**) and LNLP to
1058 HNHP (**j**). Data were obtained after cells were acclimated to experimental conditions
1059 for 14–16 generations and means ± sd of 4 replicate populations. Horizontal lines in
1060 panels (**e**)–(**j**) showed the value of 1. Different letters (a, b, c) in panels (**a**)–(**d**)
1061 represent significant differences between different nutrient treatments (Tukey Post
1062 hoc, $p < 0.05$). The results shown in the black column were used for the ambient-
1063 future comparison in figure 2. Detailed experimental conditions were shown in Figure
1064 1.

1065

1066 **Figure S1.** Flow chart of the experimental processes. Experimental steps were done in
1067 a consecutive manner. Detailed experimental conditions were shown in Figure 1.

1068

1069 **Figure S2.** Representative curves for the time course for cell concentrations of *E.*
1070 *huxleyi* under low pCO_2 (LC), high (HT) or low (LT) temperatures, and high light
1071 (HL) conditions with varying levels of nutrients: HNHP (**a**), LNHP (**b**), HNLP (**c**) and
1072 LNLP (**d**), respectively. Arrow indicates the day when samples were taken in each
1073 treatment. Data were means ± sd of 4 replicate populations. Detailed experimental
1074 conditions were shown in Figure 1.
1075
1076 **Figure S3.** Comparison of growth rate (**a**), POC quota (**b**) and PIC quota (**c**) between
1077 the expected (calculated) values and the measured values under the LNLP treatments.
1078 Different letters (a, b) in each "baseline" environment (LCLT, HCLT, LCHT or
1079 HCHT) represent significant differences (Tukey Post hoc, $p < 0.05$). Detailed
1080 experimental conditions were shown in Figure 1.
1081
1082 **Figure S4.** Heatmap of the changes in growth rate, POC quota, PIC quota and
1083 PIC:POC in each treatment. Values in the present scenario (LC LT LL HNHP) were
1084 considered as the control. A minus sign indicates the reduction in these parameters.
1085
1086 **Figure S5.** Cell volume of *E. huxleyi* grown in LCLT (**a**), HCLT (**b**), LCHT (**c**) and
1087 HCHT (**d**) conditions, and its correlation with POC quota (**e**) and PIC quota (**f**). Data
1088 were obtained after cells were acclimated to experimental conditions for 14–16
1089 generations and means ± sd of 4 replicate populations in panels (**a**)–(**d**). Each point in
1090 panels (**e**) and (**f**) indicates an individual replicate from all experiment. Different
1091 letters (a, b, c) in panels (**a**)–(**d**) represent significant differences between different
1092 nutrient treatments (Tukey Post hoc, $p < 0.05$).
1093

1094 **Figure S6.** Normalized POC quota of *E. huxleyi* to cell volume in LCLT (**a**), HCLT
1095 (**b**), LCHT (**c**) and HCHT (**d**) conditions. Data were obtained after cells were
1096 acclimated to experimental conditions for 14–16 generations and means ± sd of 4
1097 replicate populations. Different letters (a, b) in each panel represent significant
1098 differences between different nutrient treatments (Tukey Post hoc, $p < 0.05$).
1099

1100 **Figure S7.** Normalized PIC quota of *E. huxleyi* to cell volume in LCLT (**a**), HCLT
1101 (**b**), LCHT (**c**) and HCHT (**d**) conditions. Data were obtained after cells were
1102 acclimated to experimental conditions for 14–16 generations and means ± sd of 4
1103 replicate populations. Different letters (a, b, c) in each panel represent significant
1104 differences between different nutrient treatments (Tukey Post hoc, $p < 0.05$).
1105

1106 **Figure S8.** POC production rate of *E. huxleyi* in LCLT (**a**), HCLT (**b**), LCHT (**c**) and
1107 HCHT (**d**) conditions, and the ratio of POC production rate at HC to LC (**e**), HT to LT
1108 (**f**), HCHT to LCLT (**g**), LNHP to HNHP (**h**), HNLP to HNHP (**i**) and LNLP to
1109 HNHP (**j**). Data were obtained after cells were acclimated to experimental conditions
1110 for 14–16 generations and means ± sd of 4 replicate populations. Horizontal lines in
1111 panels (**e**)–(**j**) showed the value of 1. Different letters (a, b, c) in panels (**a**)–(**d**)
1112 represent significant differences between different nutrient treatments (Tukey Post
1113 hoc, $p < 0.05$).
1114

1115 **Figure S9.** PIC production rate of *E. huxleyi* in LCLT (**a**), HCLT (**b**), LCHT (**c**) and
1116 HCHT (**d**) conditions, and the ratio of PIC production rate at HC to LC (**e**), HT to LT
1117 (**f**), HCHT to LCLT (**g**), LNHP to HNHP (**h**), HNLP to HNHP (**i**) and LNLP to
1118 HNHP (**j**). Data were obtained after cells were acclimated to experimental conditions

1119 for 14–16 generations and means ± sd of 4 replicate populations. Horizontal lines in
1120 panels (**e**)–(**j**) showed the value of 1. Different letters (a, b, c) in panels (**a**)–(**d**)
1121 represent significant differences between different nutrient treatments (Tukey Post
1122 hoc, $p < 0.05$).
1123
1124 **Figure S10.** PON quota of *E. huxleyi* in LCLT (**a**), HCLT (**b**), LCHT (**c**) and HCHT
1125 (**d**) conditions, and the ratio of PON quota at HC to LC (**e**), HT to LT (**f**), HCHT to
1126 LCLT (**g**), LNHP to HNHP (**h**), HNLP to HNHP (**i**) and LNLP to HNHP (**j**). Data
1127 were obtained after cells were acclimated to experimental conditions for 14–16
1128 generations and means ± sd of 4 replicate populations. Horizontal lines in panels (**e**)–
1129 (**j**) showed the value of 1. Different letters (a, b) in panels (**a**)–(**d**) represent significant
1130 differences between different nutrient treatments (Tukey Post hoc, $p < 0.05$).
1131
1132 **Figure S11.** Normalized RNA quota of *E. huxleyi* to POC quota in HNHP and HNLP
1133 conditions. Data were obtained after cells were acclimated to experimental conditions
1134 for 14–16 generations and means ± sd of 4 replicate populations. Different letters (a, b)
1135 represent significant differences between different nutrient treatments (Tukey Post
1136 hoc, $p < 0.05$).
1137
1138

1139 **Table 1.** Carbonate chemistry parameters at the end of the incubation. The values are
1140 means ± sd of 4 replicate populations. LL and HL represent 60 and 240 µmol photons
1141 m^{-2} s^{-1} of photosynthetically active radiation (PAR), respectively; HN and LN
1142 represent 24.3 and 7.8 µmol L^{-1} DIN in the beginning of the incubation; HP and LP
1143 represent 1.5 and 0.5 µmol L^{-1} DIP in the beginning of the incubation, respectively.

			pCO_2 (µatm)	pH (total scale)	TA (µmol L^{-1})	DIC (µmol L^{-1})	HCO_3^- (µmol L^{-1})	CO_3^{2-} (µmol L^{-1})	CO_2 (µmol L^{-1})
16	LL-HNHP	LC	371±17	8.07±0.02	2266±19	2017±9	1823±6	180±8	13.4±0.6
		HC	918±21	7.73±0.02	2248±45	2149±39	2027±35	90±5	33.3±0.7
	HL-HNHP	LC	387±22	8.06±0.02	2297±12	2050±17	1857±20	179±6	14.0±0.8
		HC	972±11	7.71±0.01	2283±34	2189±31	2066±29	88±3	35.2±0.4
	HL-LNHP	LC	393±20	8.05±0.02	2273±9	2033±3	1845±9	174±7	14.3±0.7
		HC	1012±13	7.69±0.01	2263±28	2177±25	2057±24	84±2	36.7±0.5
	HL-HNLP	LC	395±19	8.06±0.02	2318±5	2073±12	1879±16	179±6	14.3±0.7
		HC	958±63	7.70±0.01	2205±69	2117±71	1999±69	84±1	34.7±2.3
	HL-LNLP	LC	375±24	8.06±0.01	2181±78	1947±77	1767±73	167±3	13.6±0.9
		HC	1014±46	7.68±0.01	2198±73	2118±73	2002±69	79±2	36.7±1.7
20	LL-HNHP	LC	349±16	8.09±0.02	2257±14	1963±4	1741±6	210±8	11.3±0.5
		HC	899±40	7.74±0.02	2257±53	2130±45	1994±40	107±7	29.0±1.3
	HL-HNHP	LC	363±11	8.08±0.01	2281±16	1990±18	1770±19	208±2	11.7±0.3
		HC	947±24	7.72±0.01	2248±21	2130±19	1998±18	102±3	30.6±0.8
	HL-LNHP	LC	362±18	8.08±0.02	2262±12	1973±13	1756±16	206±7	11.7±0.6
		HC	970±10	7.71±0.01	2271±31	2155±28	2021±25	102±3	31.4±0.3
	HL-HNLP	LC	370±14	8.08±0.01	2314±3	2023±10	1800±14	211±4	12.0±0.4
		HC	946±47	7.71±0.01	2200±72	2088±72	1960±68	98±2	30.6±1.5
	HL-LNLP	LC	350±18	8.08±0.01	2193±71	1912±68	1701±63	200±5	11.3±0.6
		HC	977±59	7.70±0.01	2192±78	2086±79	1959±76	95±2	31.6±1.9

1144
1145
1146
1147
1148
1149
1150
1151
1152

Table 2. Final nitrate and phosphate concentrations (N : P, μmol L^{-1}), growth rate (d^{-1}), POC and PIC quotas (pg C $cell^{-1}$), and PIC / POC value. Values in the brackets represent final DIN and DIP concentrations, and standard deviation of 4 replicate populations for growth rate, POC and PIC quotas, and PIC / POC value. Detailed information was shown in Table 1.

pCO_2	T	Light	Final N : P	Growth rate	POC quota	PIC quota	PIC/POC
LC	LT	LL	HNHP (17.1 : 0.7)	0.96 (0.012)	1.80 (0.14)	0.38 (0.09)	0.21 (0.07)
		HL	HNHP (17.3 : 0.5)	1.09 (0.006)	2.50 (0.28)	0.62 (0.05)	0.25 (0.05)
		HL	LNHP (2.5 : 0.6)	1.00 (0.013)	2.07 (0.25)	0.90 (0.02)	0.44 (0.05)
		HL	HNLP (15.4 : 0.1)	1.08 (0.006)	2.42 (0.08)	0.83 (0.04)	0.34 (0.01)
		HL	LNLP (2.4 : 0.1)	0.99 (0.003)	2.62 (0.25)	1.62 (0.14)	0.63 (0.11)
HC	LT	LL	HNHP (18.6 : 0.9)	0.79 (0.012)	2.52 (0.33)	0.26 (0.06)	0.10 (0.04)
		HL	HNHP (18.2 : 0.5)	1.04 (0.012)	2.85 (0.36)	0.41 (0.06)	0.15 (0.04)
		HL	LNHP (2.0 : 0.6)	0.92 (0.026)	2.75 (0.23)	0.68 (0.03)	0.25 (0.03)
		HL	HNLP (15.5 : 0.1)	0.85 (0.002)	5.06 (0.34)	0.64 (0.05)	0.13 (0.01)
		HL	LNLP (2.7 : 0.1)	0.67 (0.005)	4.91 (0.28)	0.90 (0.01)	0.18 (0.01)
LC	HT	LL	HNHP (16.6 : 0.3)	1.03 (0.006)	1.58 (0.11)	0.43 (0.02)	0.27 (0.01)
		HL	HNHP (17.3 : 0.3)	1.46 (0.004)	2.15 (0.28)	0.52 (0.07)	0.25 (0.06)
		HL	LNHP (2.1 : 0.5)	1.42 (0.004)	1.68 (0.05)	0.79 (0.04)	0.47 (0.03)
		HL	HNLP (17.0 : 0.1)	1.44 (0.004)	2.09 (0.03)	1.00 (0.05)	0.48 (0.03)
		HL	LNLP (2.1 : 0.1)	1.39 (0.038)	2.02 (0.05)	1.17 (0.13)	0.58 (0.07)
HC	HT	LL	HNHP (16.7 : 0.4)	0.99 (0.008)	1.54 (0.12)	0.34 (0.05)	0.22 (0.04)
		HL	HNHP (17.9 : 0.5)	1.43 (0.001)	2.57 (0.06)	0.42 (0.02)	0.16 (0.01)
		HL	LNHP (2.4 : 0.6)	1.38 (0.009)	1.97 (0.03)	0.52 (0.03)	0.27 (0.01)
		HL	HNLP (17.1 : 0.1)	1.27 (0.018)	3.68 (0.50)	0.74 (0.06)	0.20 (0.02)
		HL	LNLP (2.2 : 0.1)	0.87 (0.022)	3.81 (0.39)	0.89 (0.10)	0.20 (0.04)

Table 3. Results of three-way ANOVAs of the effects of temperature (T), pCO_2 (C) and light intensity (L) and their interaction on growth rate, POC and PIC quotas, and PIC / POC value. Significant values were marked in bold.

		T	C	L	T×C	T×L	C×L	T×C×L
Growth rate	F	20037.5	477.4	23625.8	120.0	1550.9	34.0	86.4
	p	**<0.01**	**<0.01**	**<0.01**	**<0.01**	**<0.01**	**<0.01**	**<0.01**
POC quota	F	27.1	54.4	62.0	7.4	1.9	< 0.1	6.1
	p	**<0.01**	**<0.01**	**<0.01**	**0.01**	0.18	0.83	**0.02**
PIC quota	F	0.4	38.6	47.6	2.3	6.6	1.6	1.1
	p	0.56	**<0.01**	**<0.01**	0.14	**0.02**	0.22	0.31
PIC / POC value	F	9.9	443.6	2.0	0.8	10.0	0.6	0.3
	p	**<0.01**	**<0.01**	0.17	0.38	**<0.01**	0.46	0.60

Table 4. Results of four-way ANOVAs of the effects of temperature (T), pCO_2 (C), dissolved inorganic nitrate (N) and phosphate (P) concentrations and their interaction on growth rate, POC and PIC quotas, and PIC / POC value. Significant values were marked in bold.

	Growth rate		POC quota		PIC quota		PIC / POC value	
	F	*p*	F	*p*	F	*p*	F	*p*
T	500026.0	**<0.01**	297.4	**<0.01**	30.2	**<0.01**	82.8	**<0.01**
C	5798.0	**<0.01**	162.8	**<0.01**	376.2	**<0.01**	787.3	**<0.01**
N	4542.0	**<0.01**	157.0	**<0.01**	84.4	**<0.01**	127.6	**<0.01**
P	5347.0	**<0.01**	206.5	**<0.01**	474.6	**<0.01**	0.1	0.74
T×C	6899.0	**<0.01**	52.2	**<0.01**	0.2	0.68	7.2	**<0.01**
T×N	510.0	**<0.01**	5.6	**0.02**	60.0	**<0.01**	7.9	**<0.01**
T×P	39.0	**<0.01**	5.2	**0.03**	9.4	**<0.01**	16.2	**<0.01**
C×N	1265.0	**<0.01**	107.2	**<0.01**	9.5	**<0.01**	3.1	0.09
C×P	1718.0	**<0.01**	174.1	**<0.01**	14.7	**<0.01**	88.0	**<0.01**
N×P	179.0	**<0.01**	19.7	**<0.01**	10.7	**<0.01**	14.3	**<0.01**
T×C×N	35.0	**<0.01**	<0.1	0.81	0.2	0.67	1.9	0.17
T×C×P	27.0	**<0.01**	5.5	**0.02**	0.1	0.71	1.0	0.31
T×N×P	96.0	**<0.01**	<0.1	0.80	15.7	**<0.01**	3.3	0.08
C×N×P	241.0	**<0.01**	0.4	0.56	8.2	**<0.01**	1.2	0.28
T×C×N×P	105.0	**<0.01**	3.9	0.05	22.4	**<0.01**	4.5	**0.04**

Table 5. List of the physiological responses of *E. huxleyi* to the concurrent changes in multiple drivers investigated by the laboratory incubations in the published studies. '↑' represents increase, '↓' represents decrease, and 'n' represents no significant change to simultaneous changes in multiple drivers. C, T, L, N, P and μ represent CO_2 (μatm), temperature (°C), light intensity (μmol photons m^{-2} s^{-1}), dissolved inorganic nitrogen and phosphate (μmol L^{-1}), and growth rate, respectively. Simultaneous changes in multiple drivers were marked in bold. [1] represents De Bodt et al., (2010), [2] Borchard et al., (2011), [3] Sett et al., (2014), [4] Gafar and Schulz, (2018), [5] Tong et al., (2019), [6] Jin et al., (2017), [7] Bretherton et al., (2019), [8] Rost et al., (2002), [9] Feng et al., (2008), [10] Müller et al. (2012), [11] Perrin et al., (2016), [12] Leonardos and Geider, (2005), [13] Matthiessen et al., (2012), [14] Zhang et al., (2019), [15] this study.

Strain	C	T	L	N	P	μ	POC	PIC	PIC: POC	Cite
AC481	**380 to 750**	**13 to 18**	150	32	1	n	↑	↓	↓	[1]
PML B92/11	**300 to 900**	**14 to 18**	300	29	1	↑	n	↓	↓	[2]
PML B92/11	**400 to 1000**	**10 to 20**	150	64	4	↑	↑	↓	↓	[3]
PML B92/11	**400 to 1000**	**10 to 20**	150	64	4	↑	↓	↓		[4]
PML B92/11	**400 to 1000**	**15 to 24**	190	100	10	↑	↑	↓	↓	[5]
CCMP2090	**395 to 1000**	20	**57 to 567**	110	10	↑	↑			[6]
NZEH	**390 to 1000**	20	**175 to 300**	100	10	↓	↑	↑	↑	[7]
PCC124-3	**390 to 1000**	20	**175 to 300**	100	10	↑	n	↑	↑	[7]
PCC70-3	**390 to 1000**	20	**175 to 300**	100	10	↑	n	↑	↑	[7]
PML B92/11	**140 to 880**	15	**80 to 150**	100	6	↑	↑	↓	↓	[8]
PML B92/11	**395 to 1000**	20	**54 to 457**	110	10	↑	↑	↓	↓	[6]
PML B92/11	**400 to 1000**	20	**50 to 1200**	64	4	↑	↑	↑		[4]
RCC962	**390 to 1000**	20	**175 to 300**	100	10	↓	↑	n	↓	[7]
CCMP371	**375 to 750**	**20 to 24**	**50 to 400**	100	10	↑	n	↓	↓	[9]
B62	**280 to 1000**	20	300	**88 to 9**	4		↑	↓	↓	[10]
RCC911	400	20	**30 to 140**	**100 to 5**	6	↑	↑	↑	↑	[11]
RCC911	400	20	**30 to 140**	100	**6 to 0.6**	↑	↑	↑	↑	[11]

PML92A	**360 to 2000**	18	**80 to 500**	200	**6.7 to 40**	n	↑			[12]
A	**460 to 1280**	16	130	**17 to 9**	**0.2 to 0.5**		↓	↓		[13]
PML B92/11	**410 to 920**	20	**80 to 480**	**100 to 8**	10	↓	↓	↑	↑	[14]
PML B92/11	**410 to 920**	20	**80 to 480**	100	**10 to 0.4**	↓	↑	n	↓	[14]
PML B92/11	**370 to 960**	**16 to 20**	**60 to 240**	**24 to 8**	**1.5 to 0.5**	↓	↑	↑	n	[15]

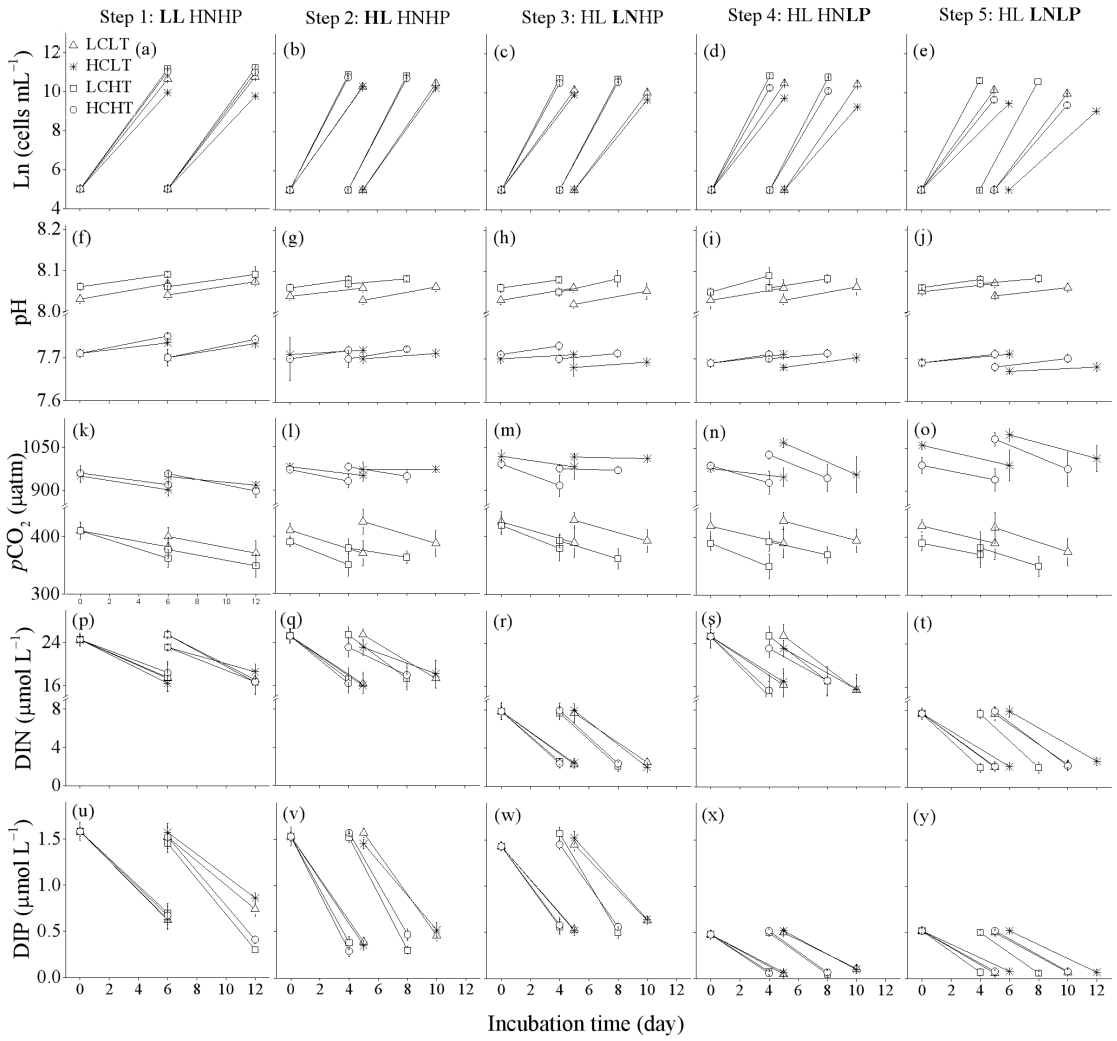
Step 1: LL HNHP
Step 2: HL HNHP
Step 3: HL LNHP
Step 4: HL HNLP
Step 5: HL LNLP
LCLT
HCLT
LCHT
HCHT
Ln (cells mL^{-1})
pH
pCO_2 (µatm)
DIN (µmol L^{-1})
DIP (µmol L^{-1})
Incubation time (day)

Figure 1

1251

1252

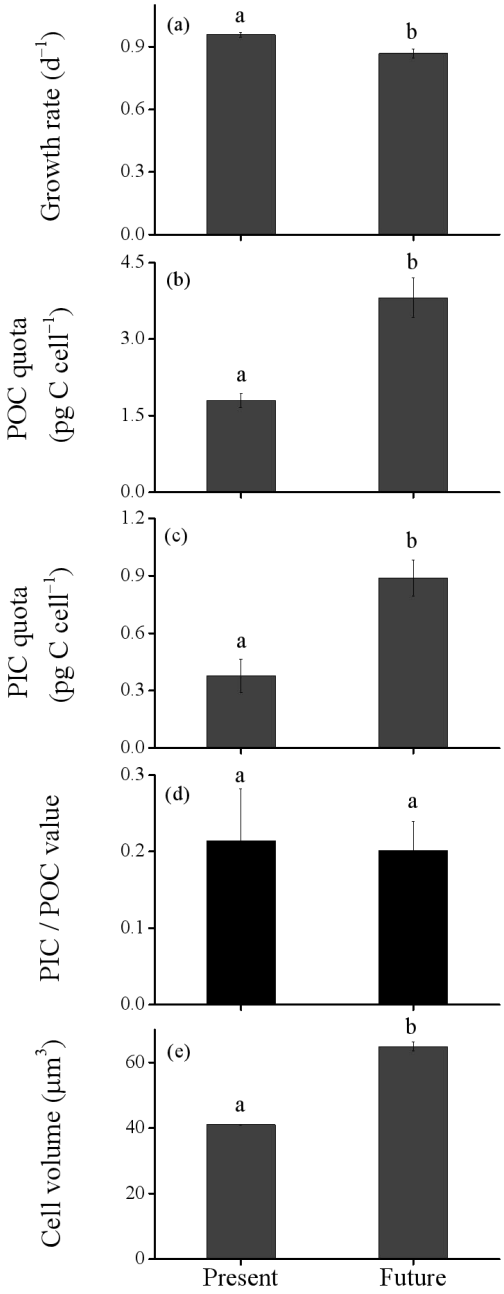

1253

1254

1255 Figure 2

1256

1257

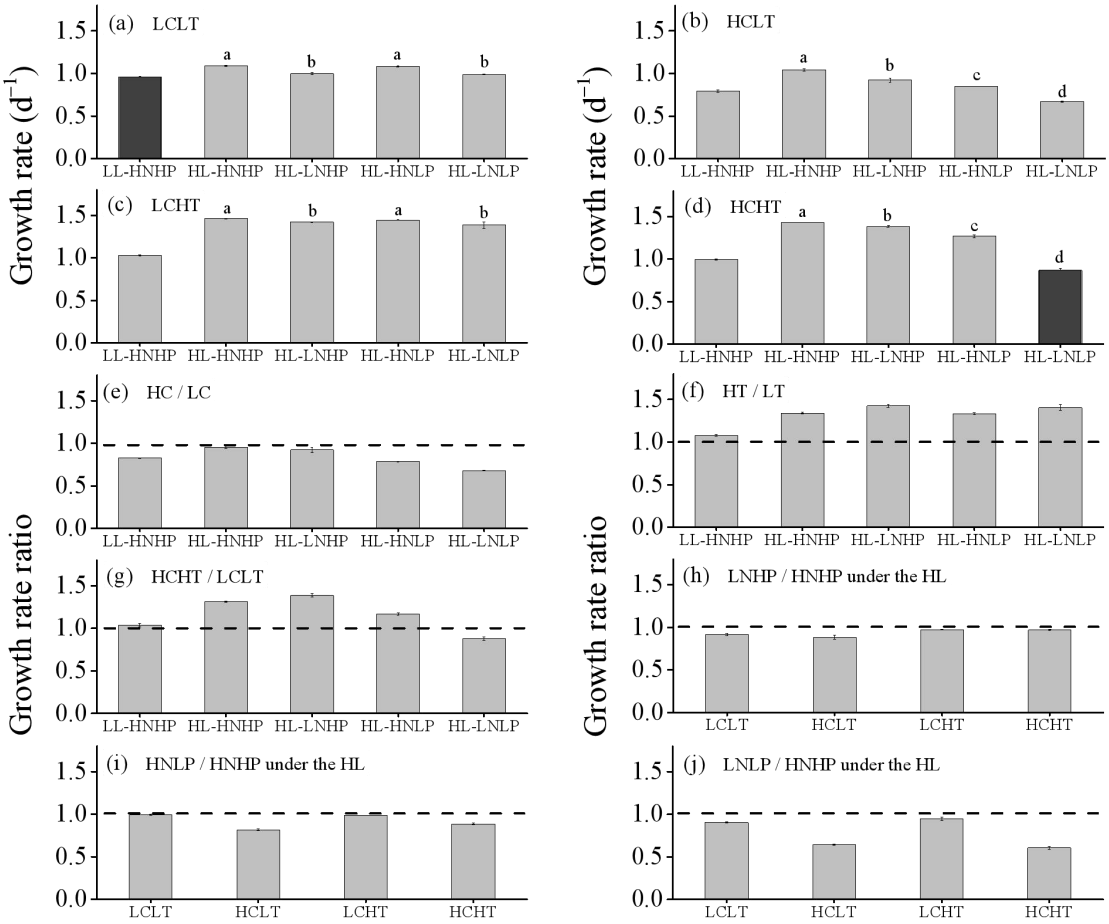
(a) LCLT
(b) HCLT
(c) LCHT
(d) HCHT
(e) HC / LC
(f) HT / LT
(g) HCHT / LCLT
(h) LNHP / HNHP under the HL
(i) HNLP / HNHP under the HL
(j) LNLP / HNHP under the HL
Growth rate (d^{-1})
Growth rate ratio
LL-HNHP
HL-HNHP
HL-LNHP
HL-HNLP
HL-LNLP
LCLT
HCLT
LCHT
HCHT

Figure 3

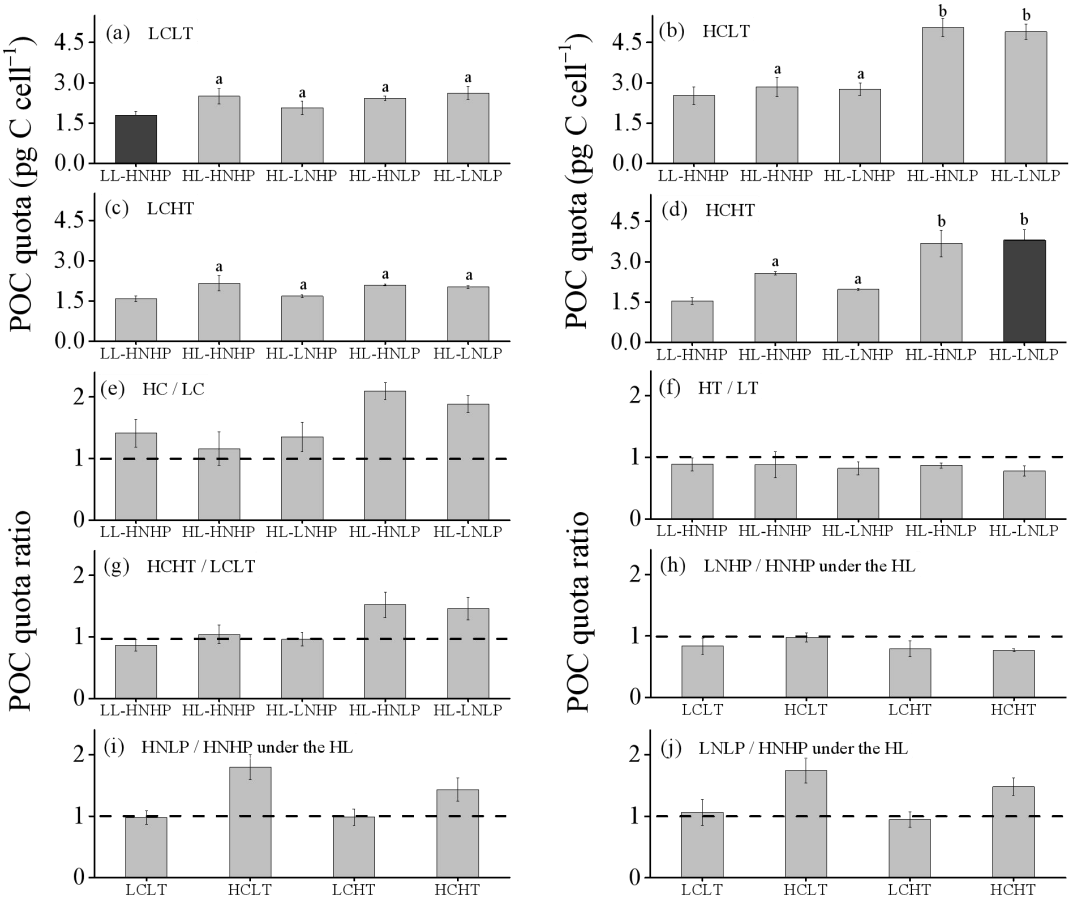
(a) LCLT
(b) HCLT
(c) LCHT
(d) HCHT
(e) HC / LC
(f) HT / LT
(g) HCHT / LCLT
(h) LNHP / HNHP under the HL
(i) HNLP / HNHP under the HL
(j) LNLP / HNHP under the HL
POC quota (pg C cell^{-1})
POC quota ratio
LL-HNHP
HL-HNHP
HL-LNHP
HL-HNLP
HL-LNLP
LCLT
HCLT
LCHT
HCHT

Figure 4

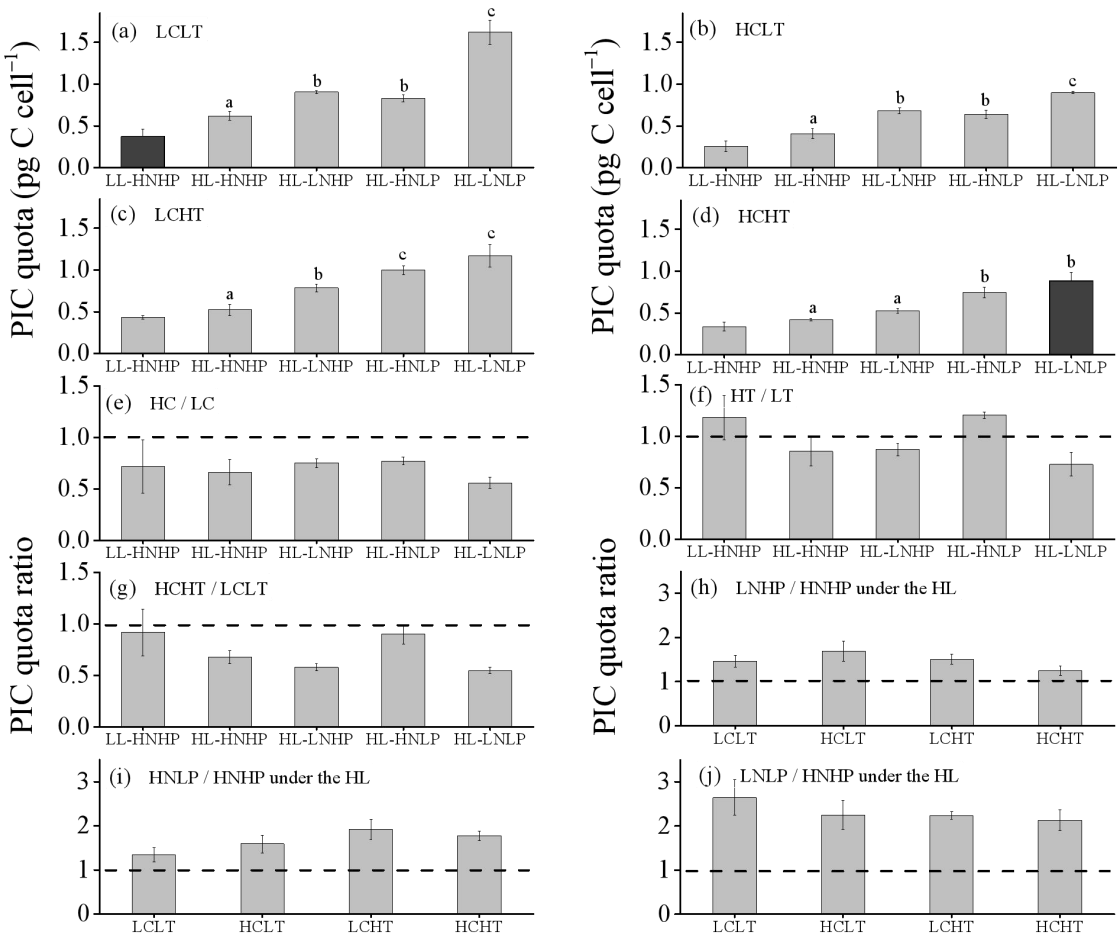
(a) LCLT
(b) HCLT
(c) LCHT
(d) HCHT
(e) HC / LC
(f) HT / LT
(g) HCHT / LCLT
(h) LNHP / HNHP under the HL
(i) HNLP / HNHP under the HL
(j) LNLP / HNHP under the HL
PIC quota (pg C cell^{-1})
PIC quota ratio
LL-HNHP
HL-HNHP
HL-LNHP
HL-HNLP
HL-LNLP
LCLT
HCLT
LCHT
HCHT

Figure 5

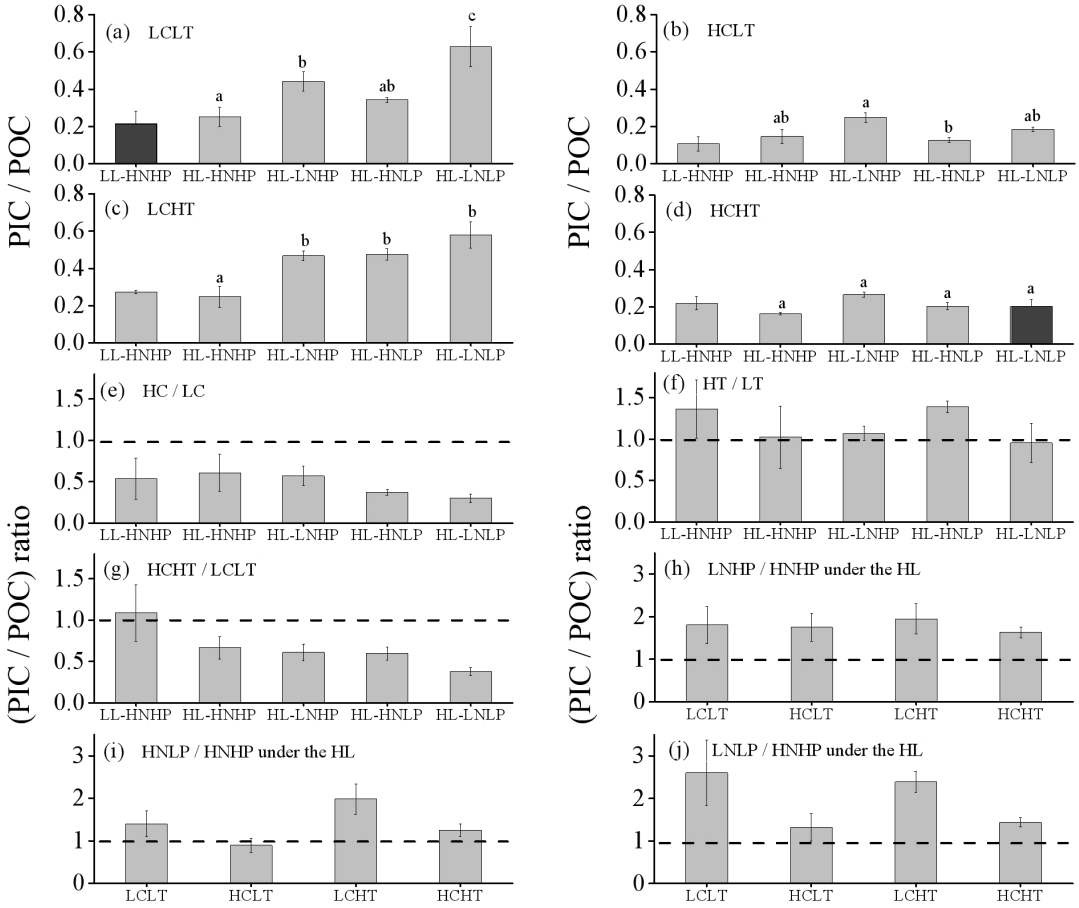
(a) LCLT
(b) HCLT
(c) LCHT
(d) HCHT
(e) HC / LC
(f) HT / LT
(g) HCHT / LCLT
(h) LNHP / HNHP under the HL
(i) HNLP / HNHP under the HL
(j) LNLP / HNHP under the HL
PIC / POC
(PIC / POC) ratio
LL-HNHP
HL-HNHP
HL-LNHP
HL-HNLP
HL-LNLP
LCLT
HCLT
LCHT
HCHT

Figure 6